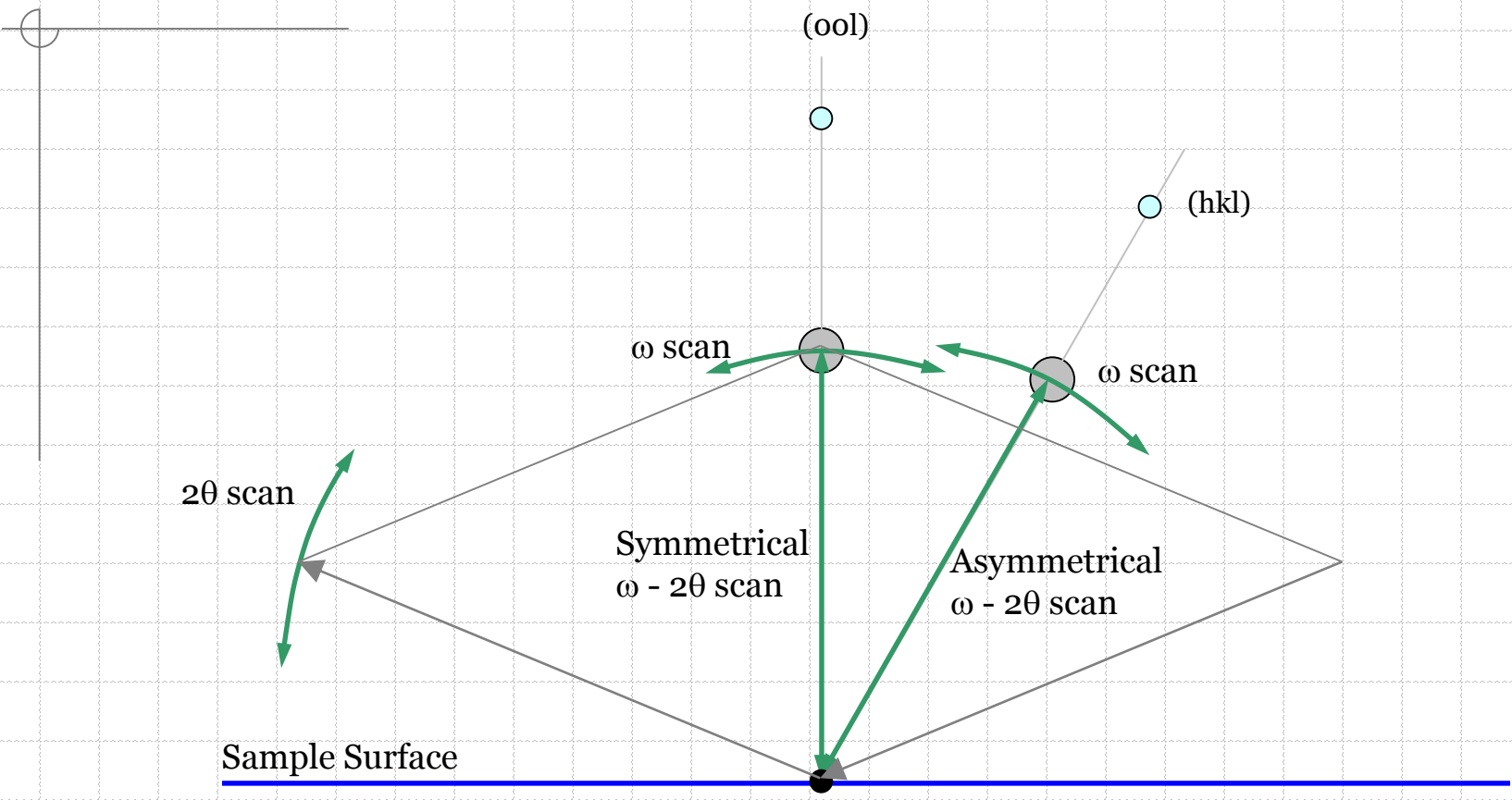


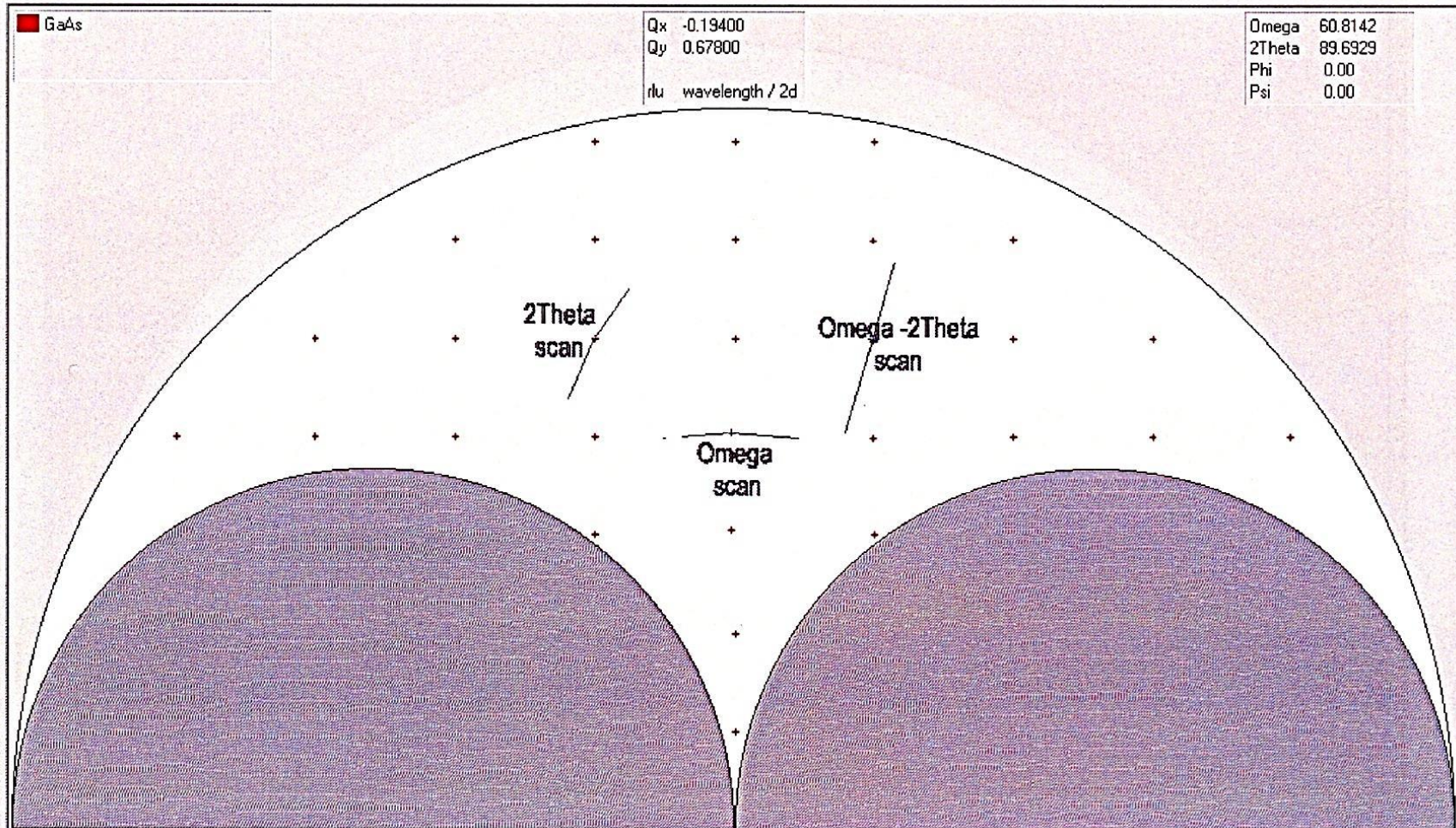
High-Resolution XRD – 2

Reciprocal Lattice Mapping
Superlattices

Scan directions



Reciprocal Space



ω -scan is in the direction of an arc centered on the origin

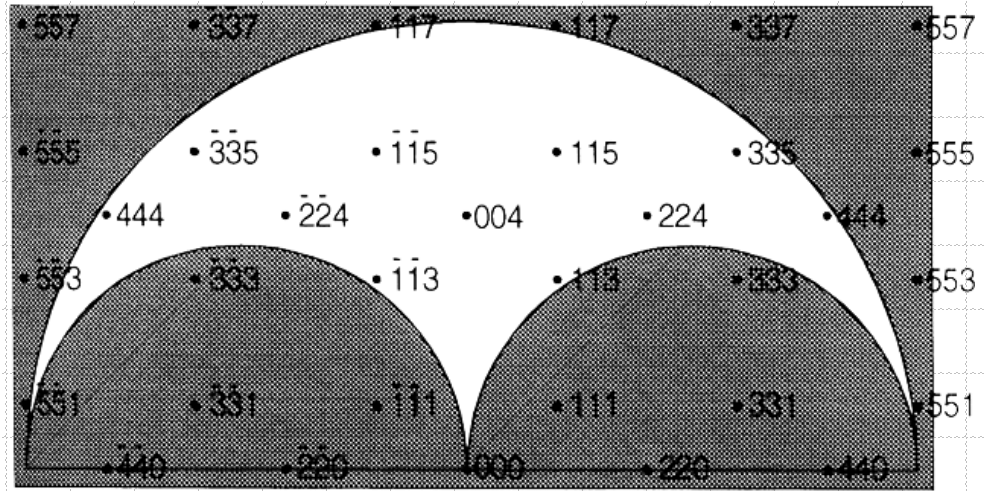
2θ -scan is an arc along Ewald sphere circumference

ω - 2θ scan is always straight line pointing away from the origin of the reciprocal space

Reciprocal Space

$$Q_x = \frac{1}{2} \{ \cos \omega - \cos(2\theta - \omega) \}$$

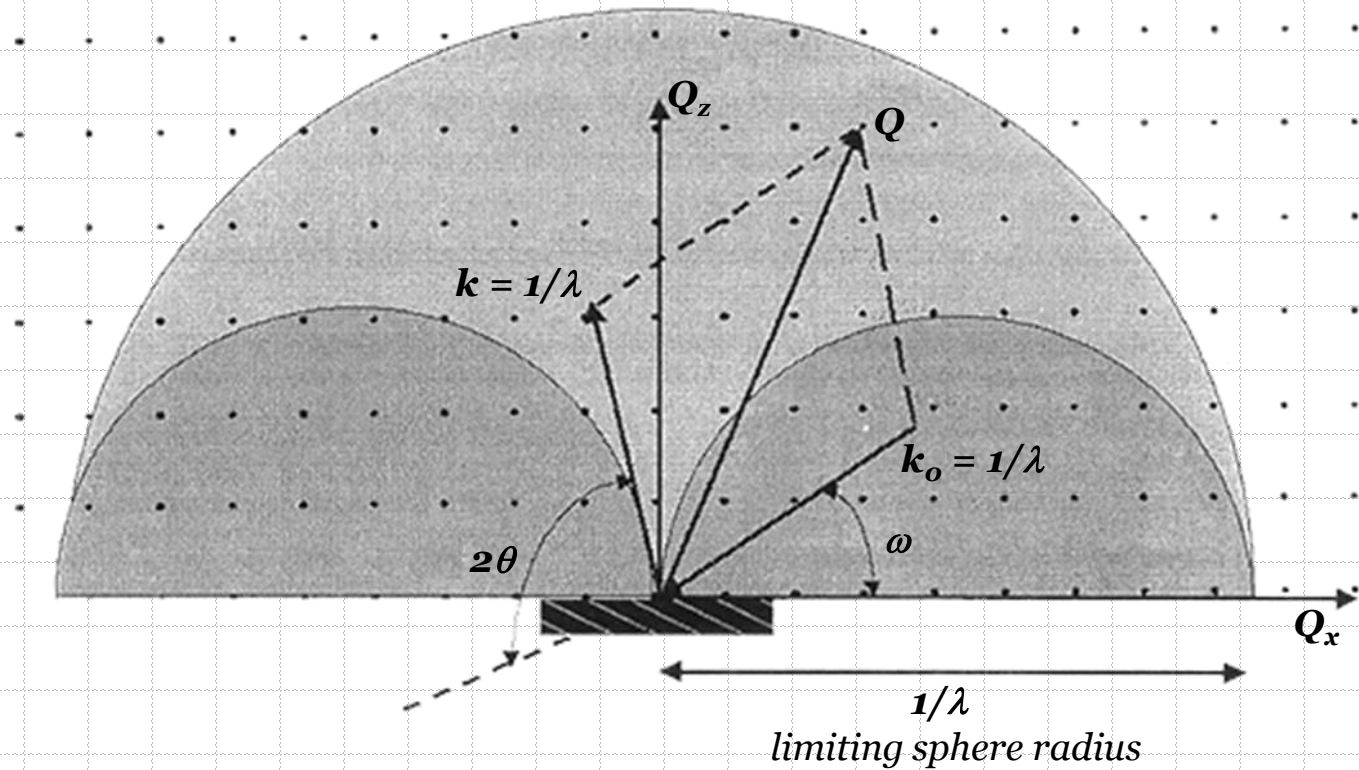
$$Q_z = \frac{1}{2} \{ \sin \omega + \sin(2\theta - \omega) \}$$



$$q = \frac{4\pi \sin \theta}{\lambda}$$

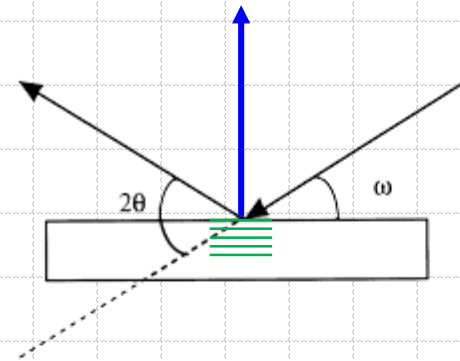
$$q_x = \frac{4\pi Q_x}{\lambda}$$

$$q_z = \frac{4\pi Q_z}{\lambda}$$



Symmetric and Asymmetric Scans

◆ Symmetric scan

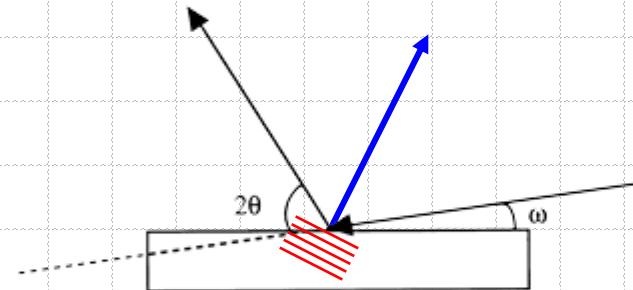


Si
a = 5.43105 Å
λ = 1.5406 Å (Cu Kα1)

(004)

ω = 34.56428 °
2θ = 69.12856 °

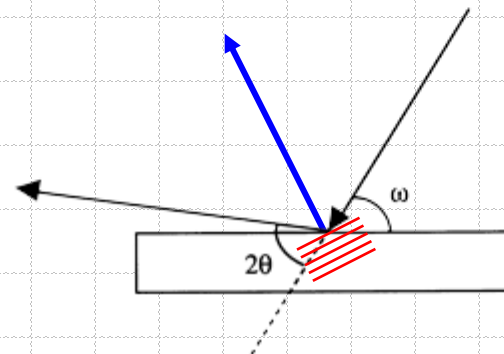
◆ Asymmetric scan. Low angle of incidence.



(113)

ω = 2.82117 °
2θ = 56.12113 °

◆ Asymmetric scan. High angle of incidence.

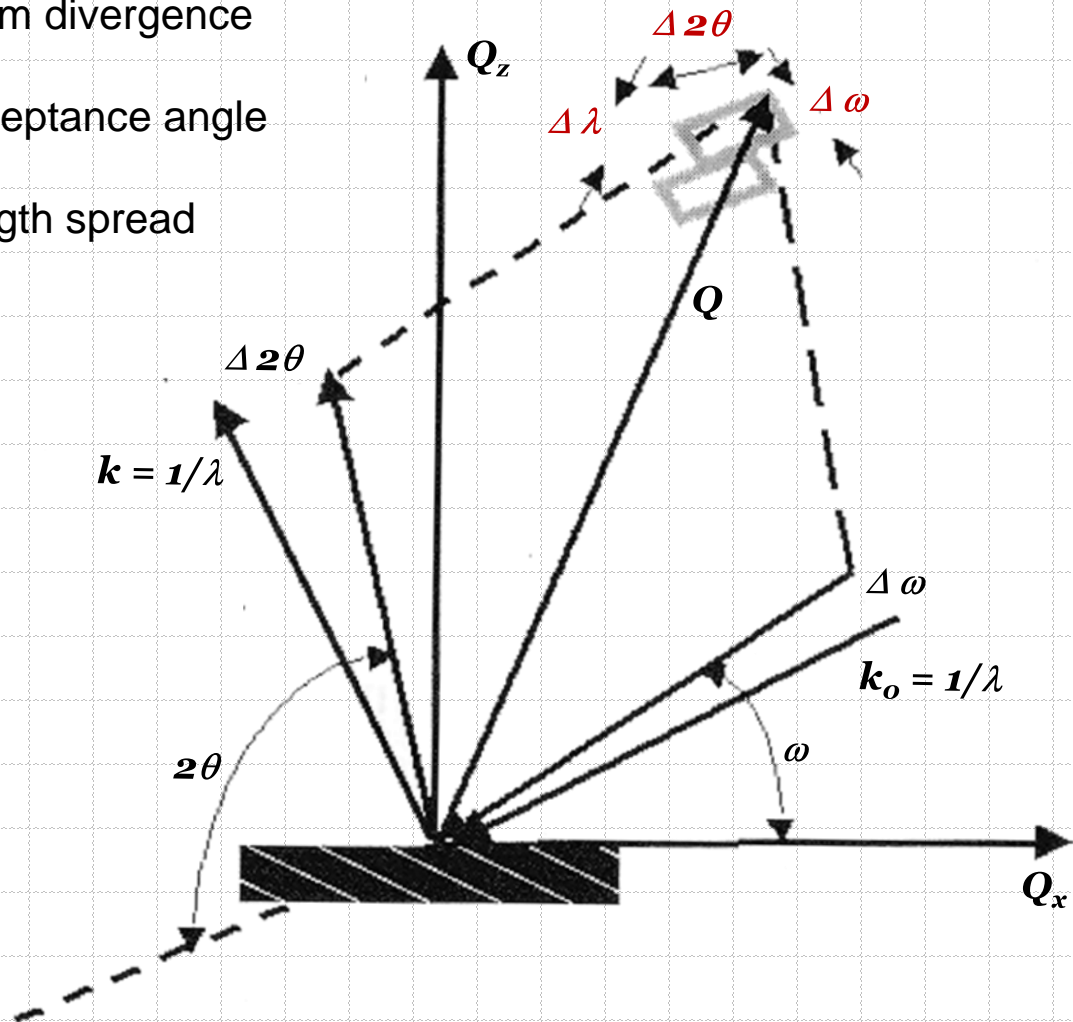


($\bar{1}\bar{1}3$)

ω = 53.29997 °
2θ = 56.12113 °

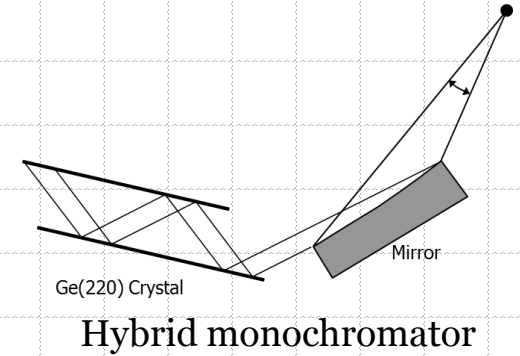
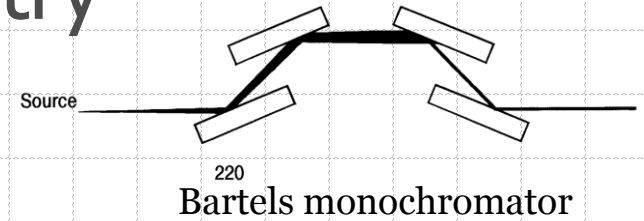
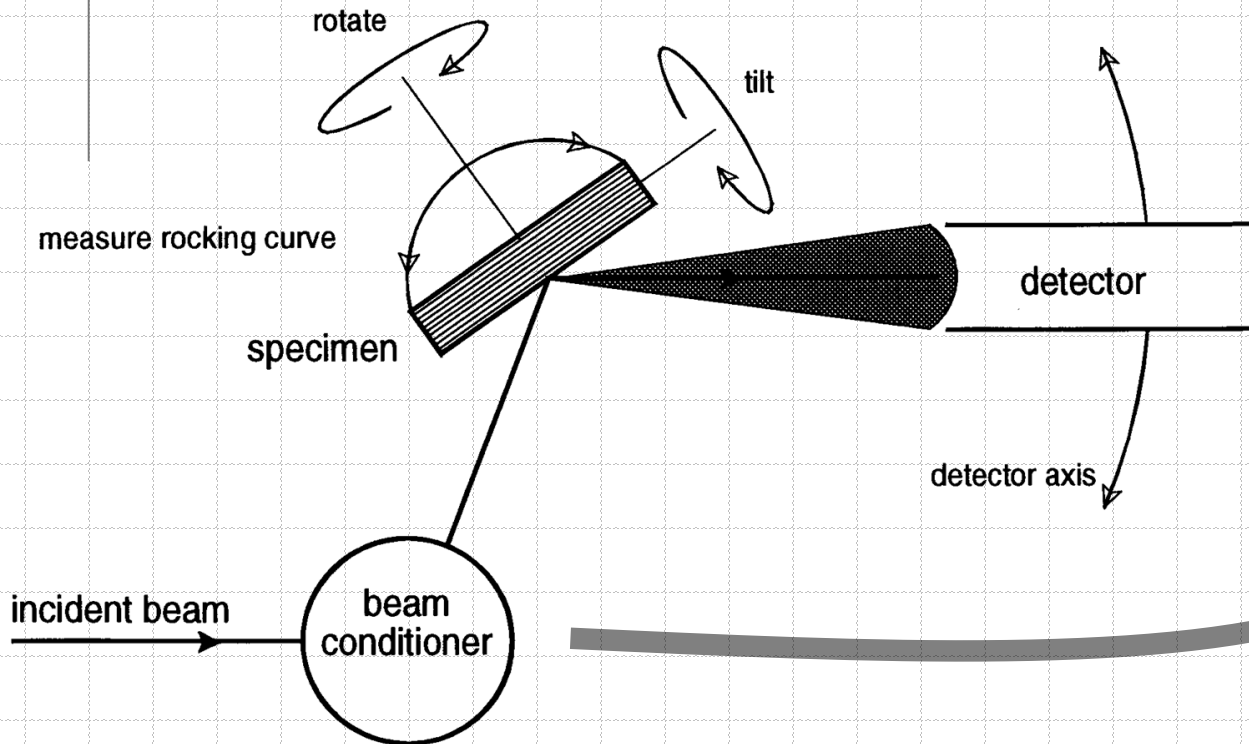
Reciprocal Space – instrument resolution

- Influence of incident beam divergence
- Influence of detector acceptance angle
- Influence of the wavelength spread

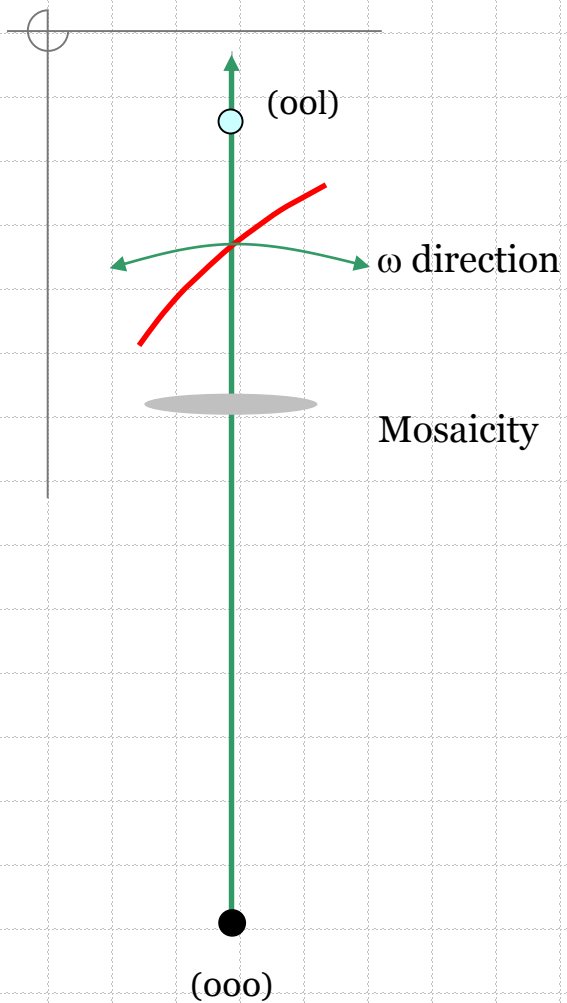


High-Resolution Diffractometry

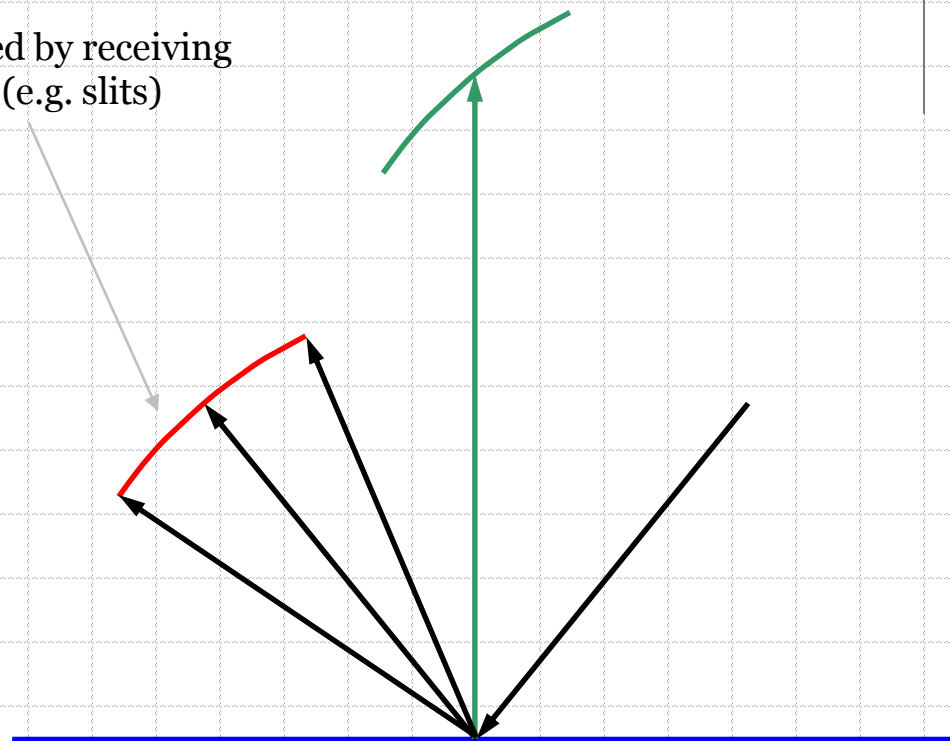
◆ Schematic of high resolution double-axis instrument



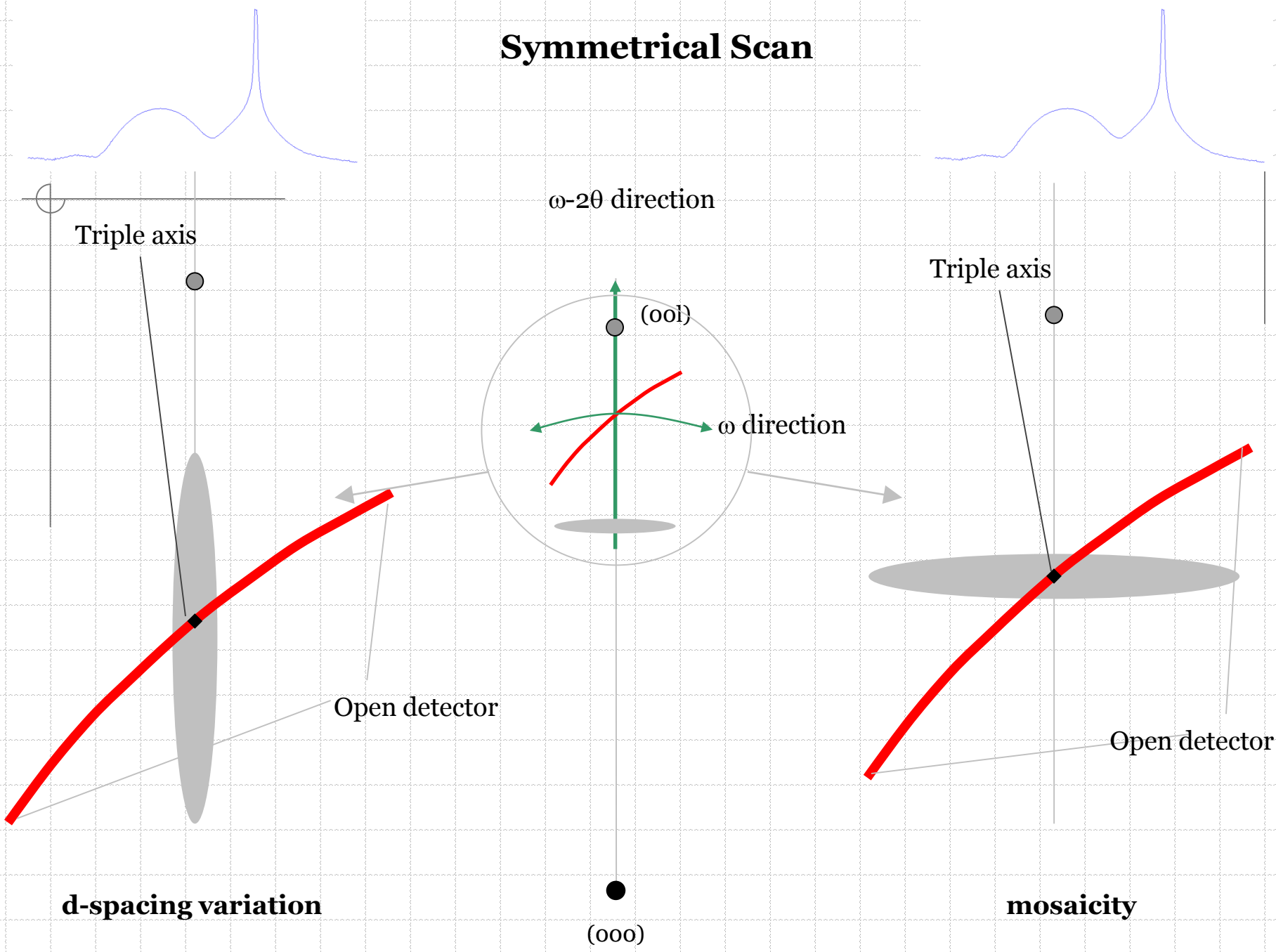
$\omega-2\theta$ direction



Defined by receiving optics (e.g. slits)

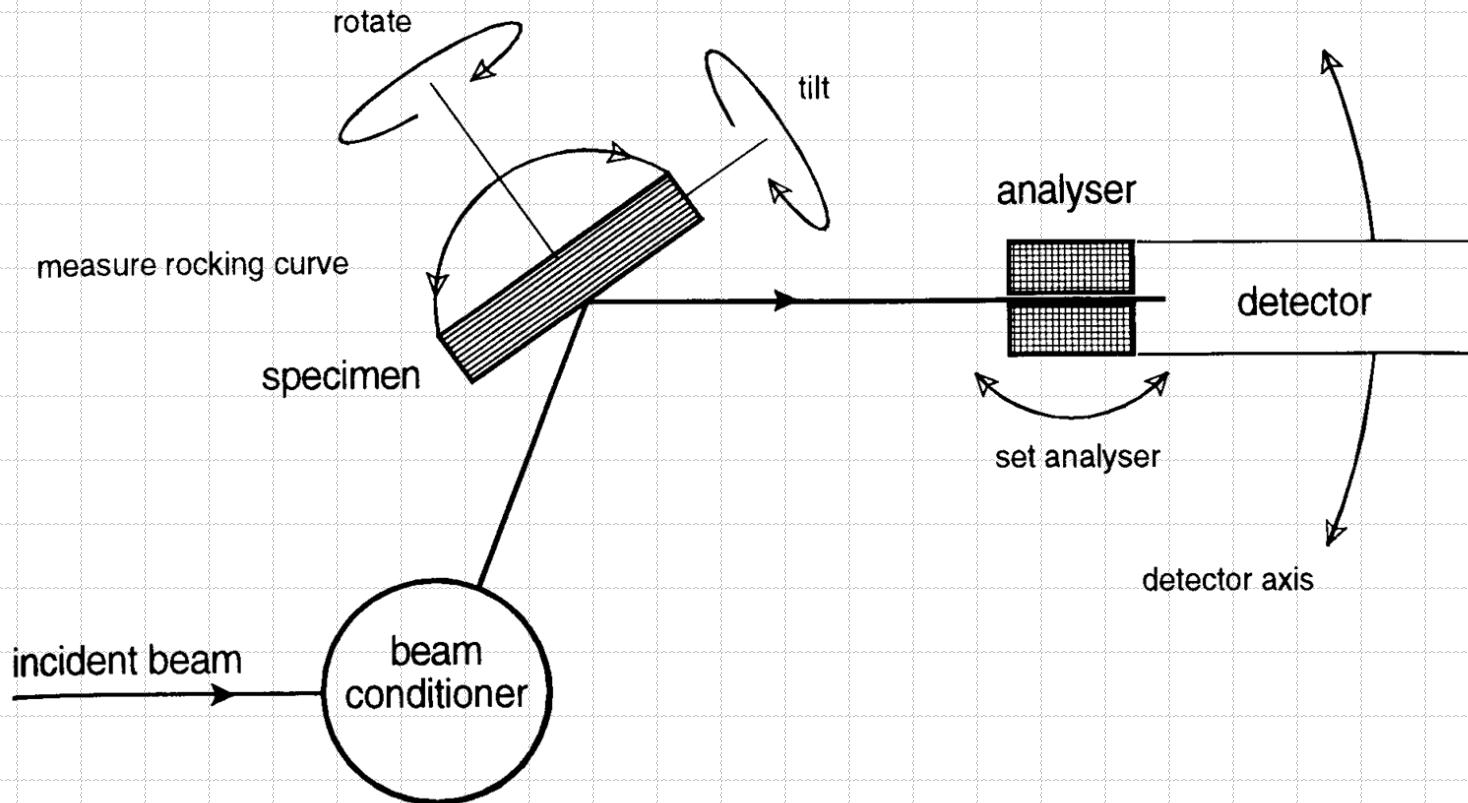


Symmetrical Scan



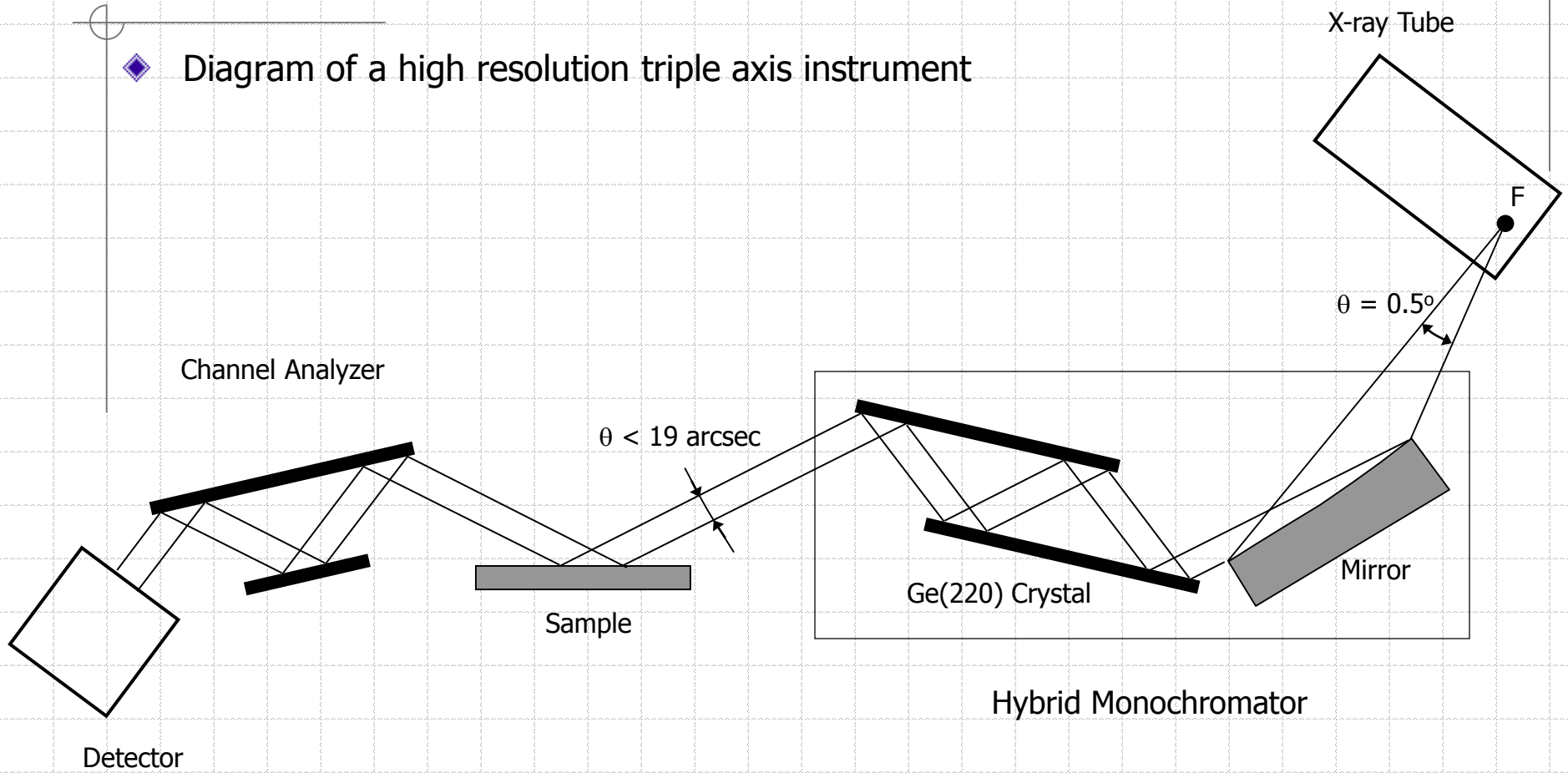
Triple Axis Geometry

◆ Schematic of high resolution triple-axis instrument

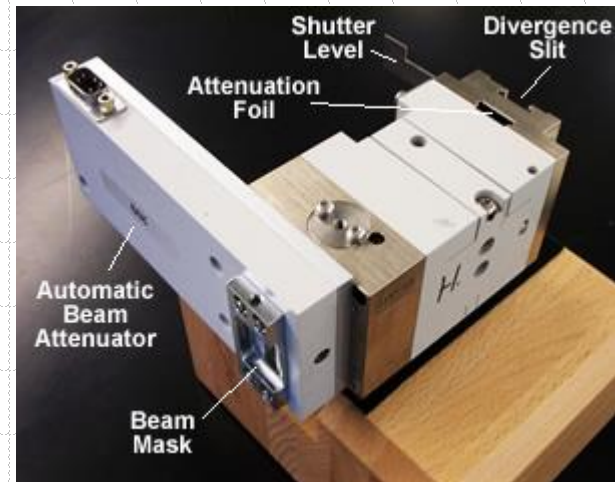
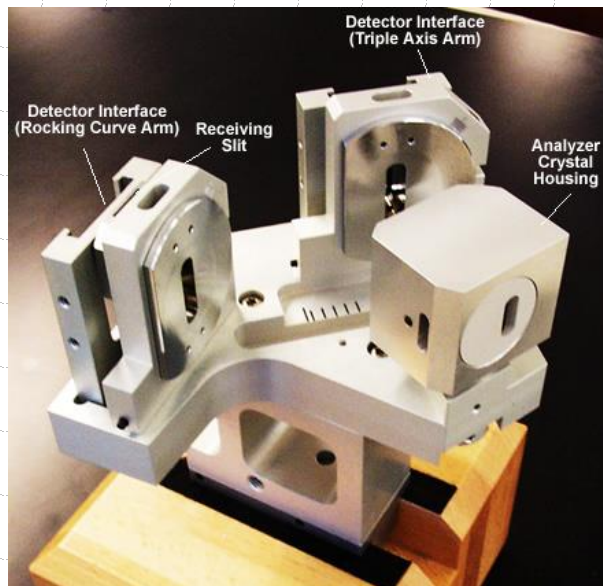
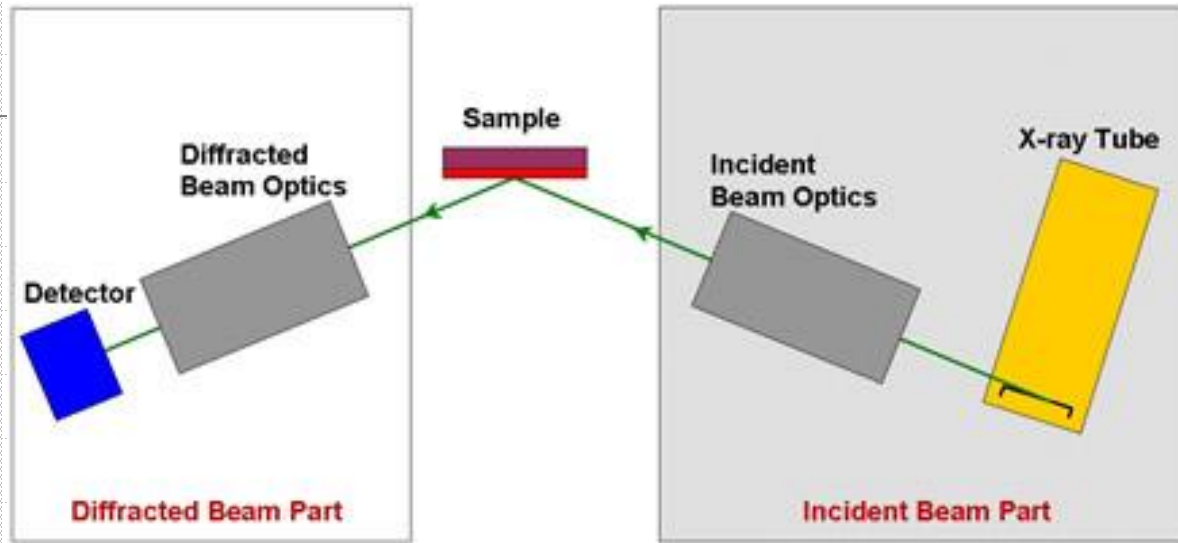


Triple Axis Geometry

◆ Diagram of a high resolution triple axis instrument

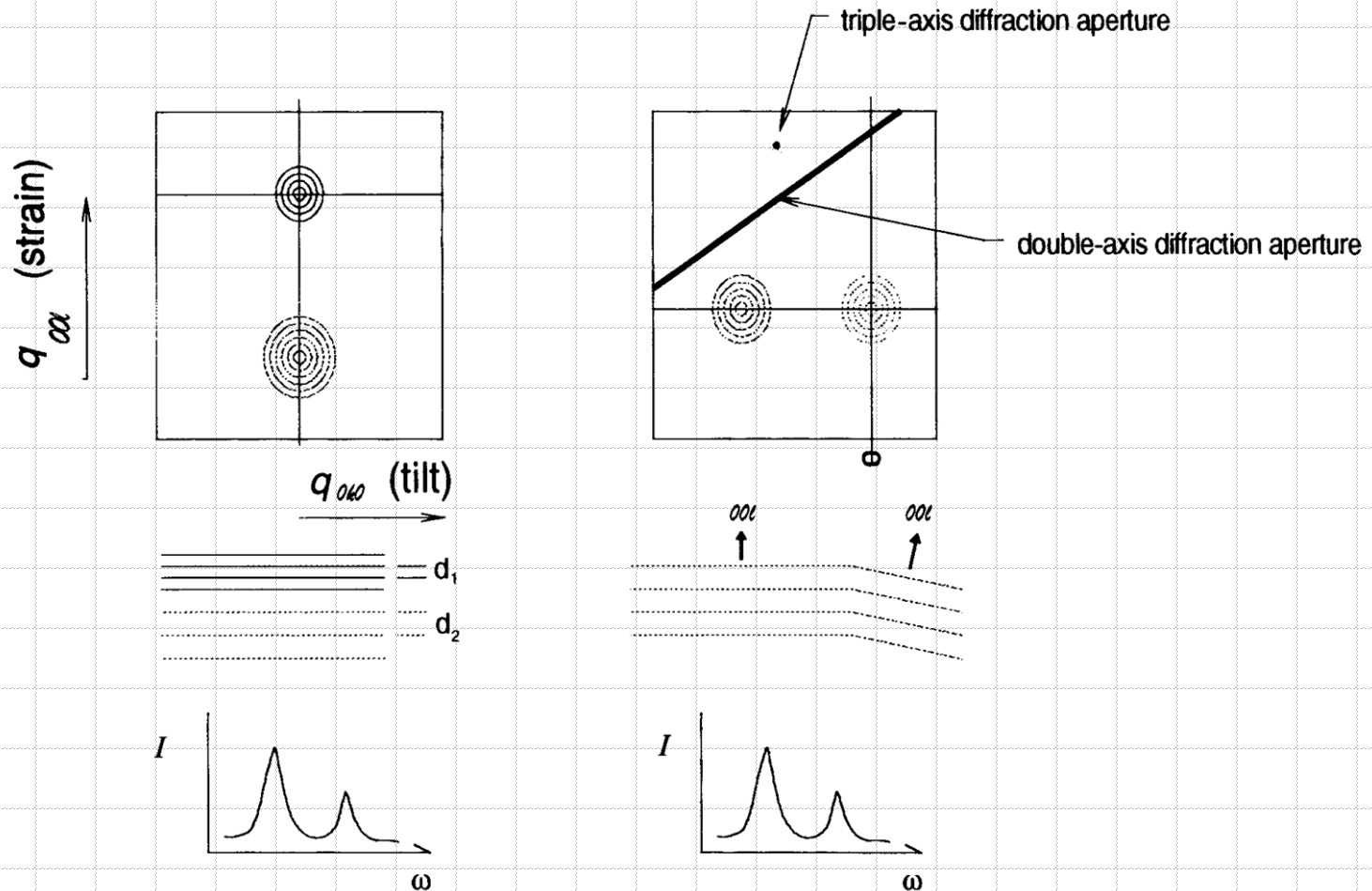


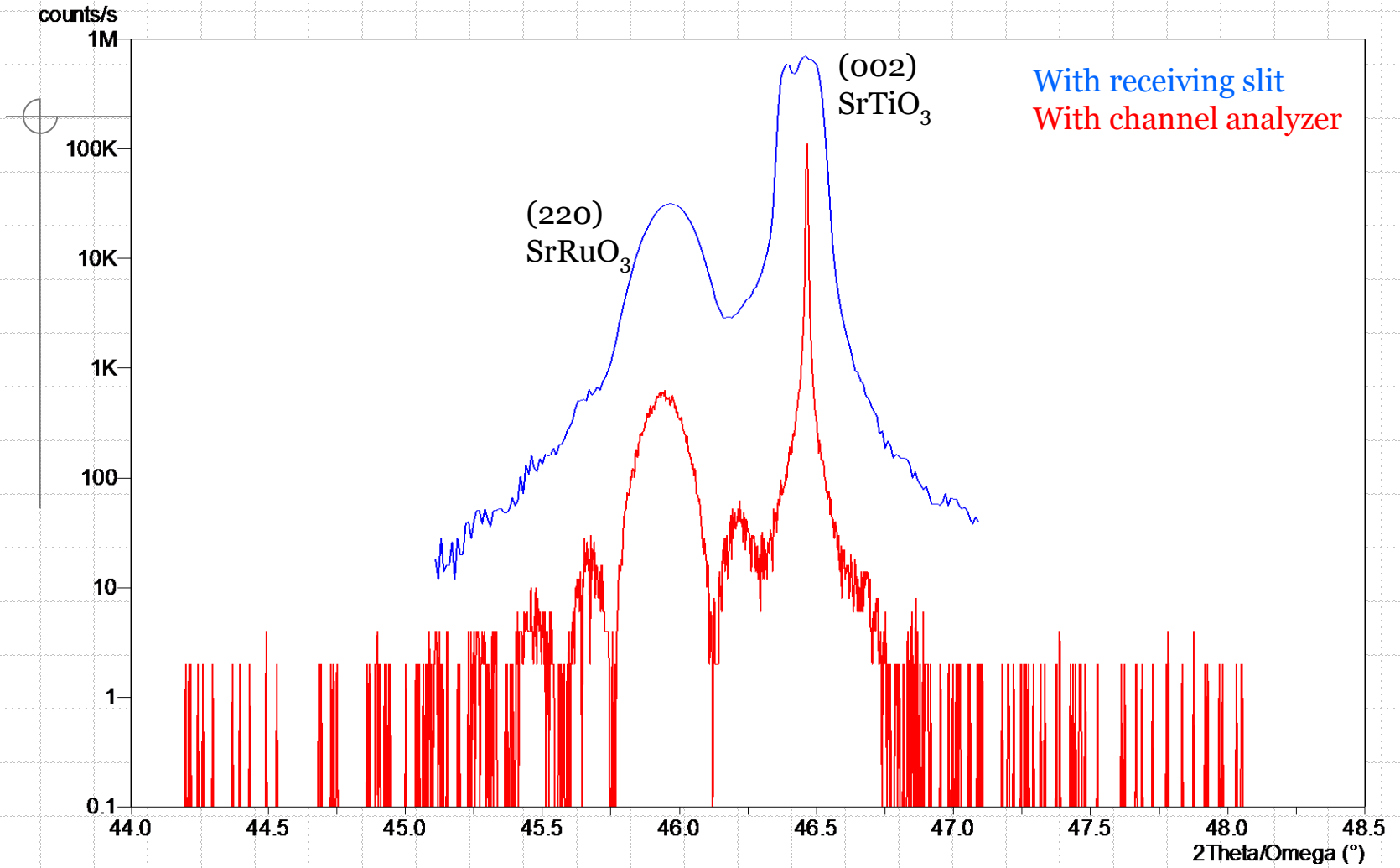
High-resolution optics



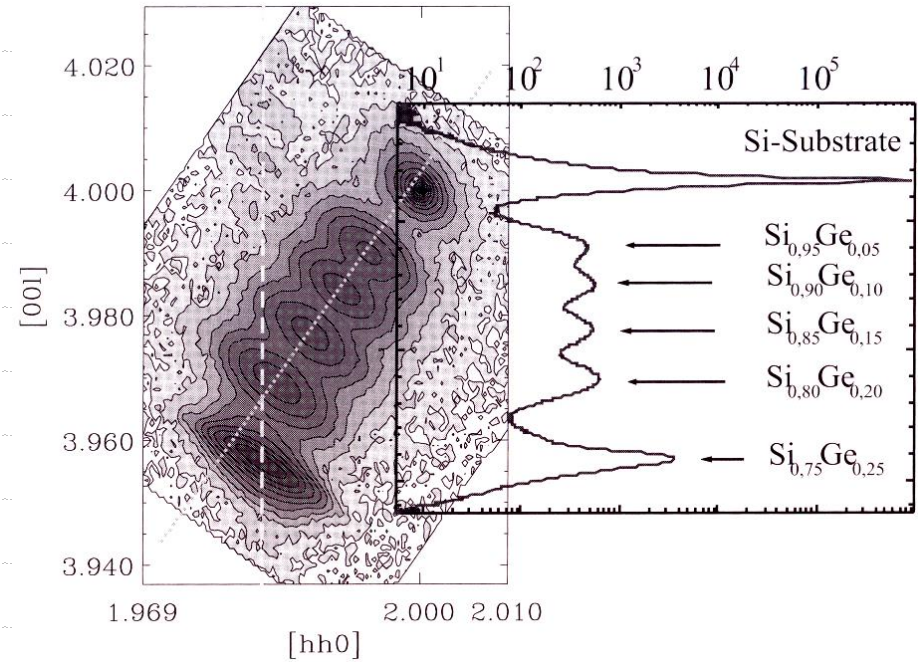
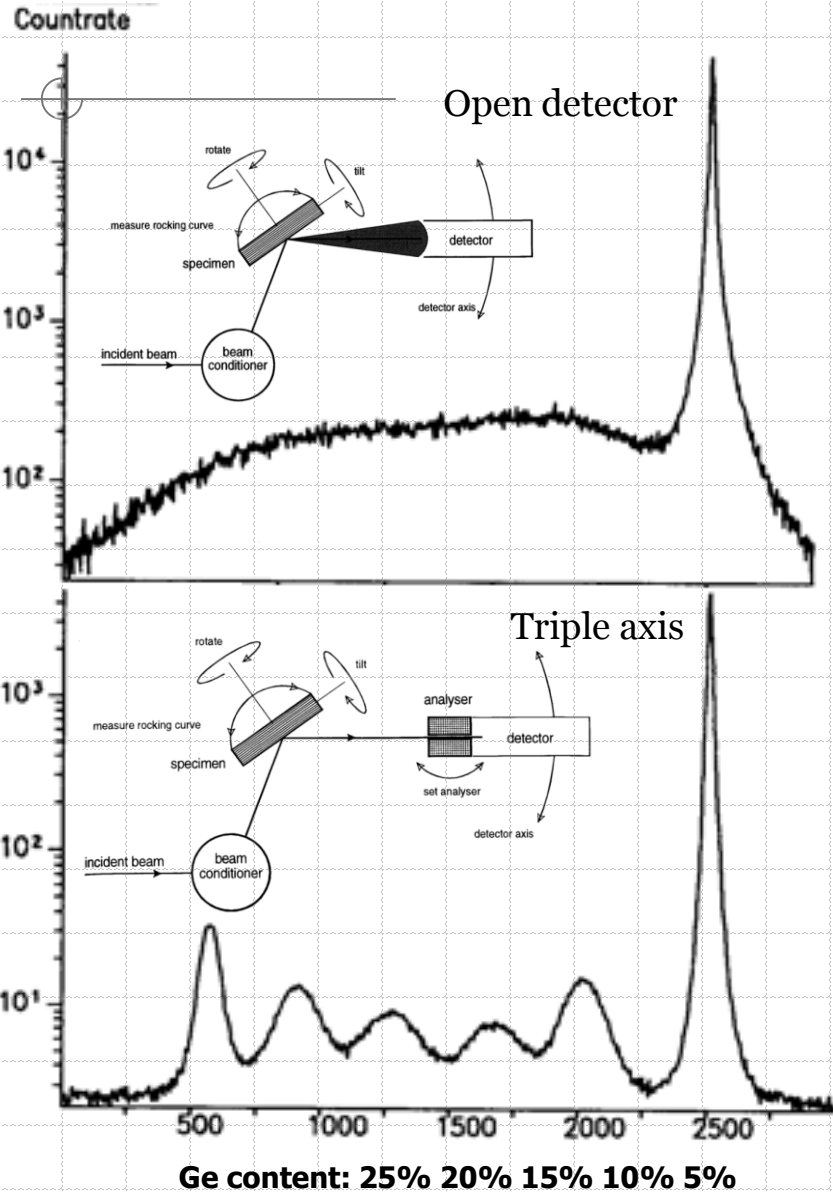
Separation of Lattice Tilts and Strains

◆ Triple axis measurements: real and reciprocal representations

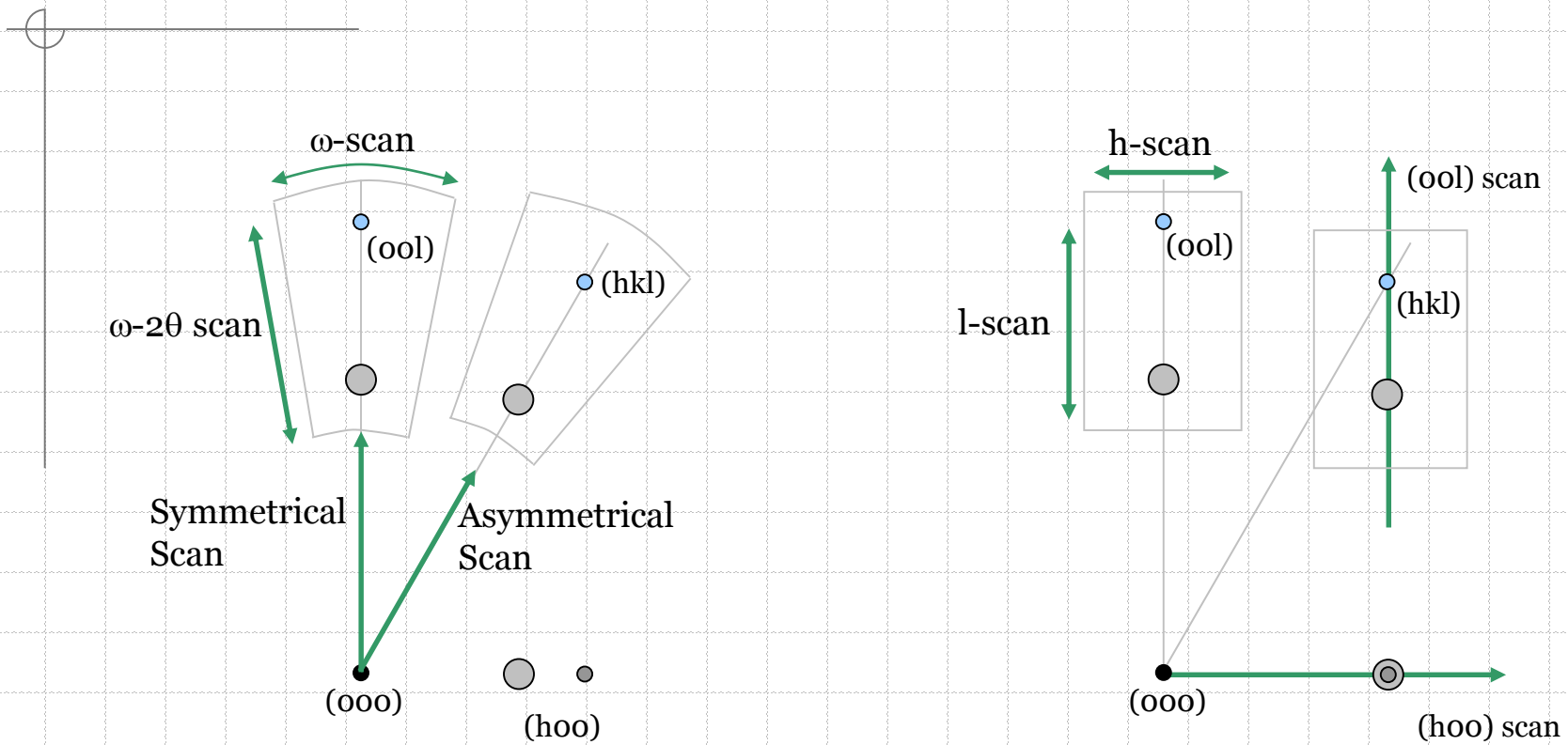




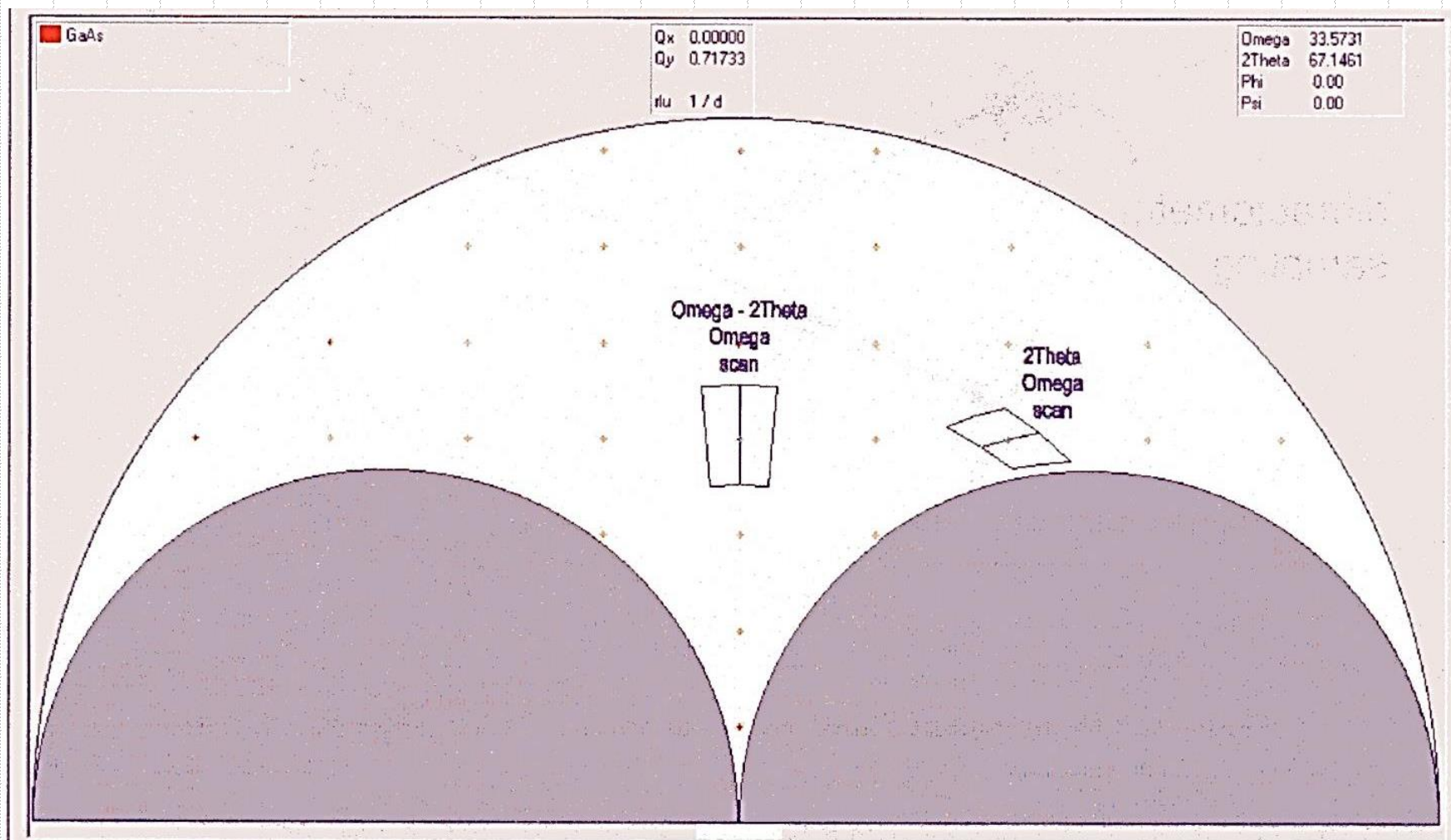
Triple-Axis Diffractometry



arcsec



Triple-Axis Diffractometry



Relaxed SiGe on Si(001)

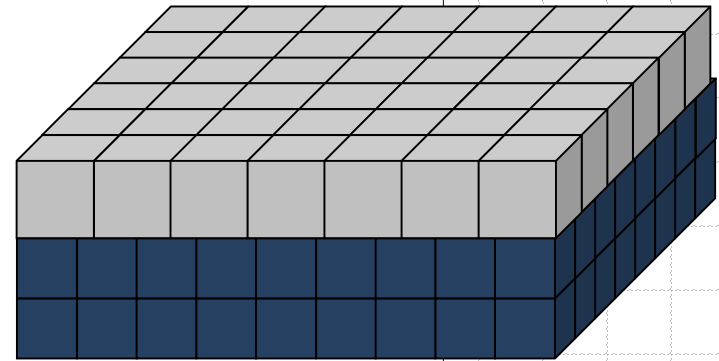
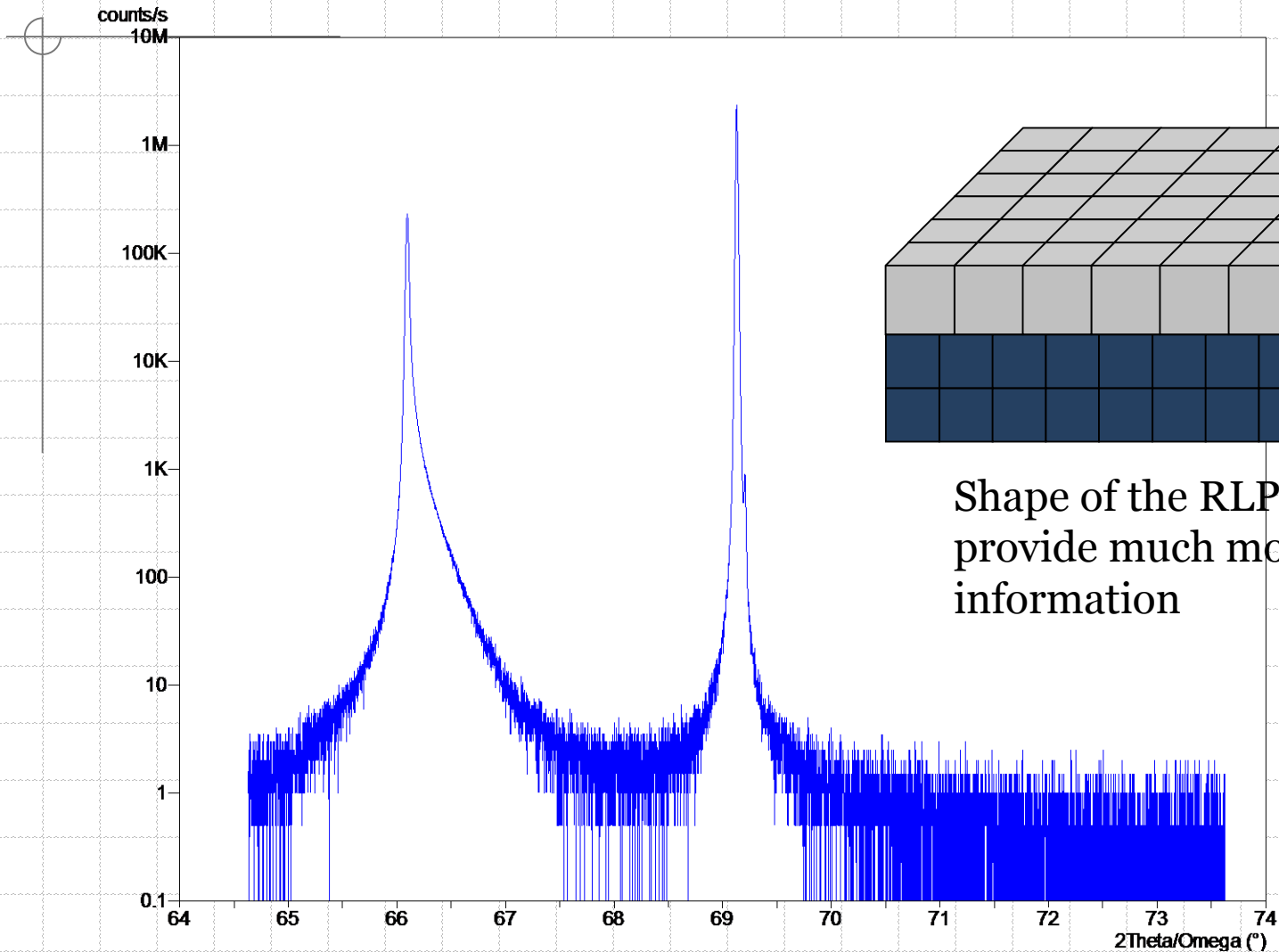
004

Omega 34.56550
2Theta 69.13090

Phi 0.00
Psi 0.00

X 0.00
Y 0.00

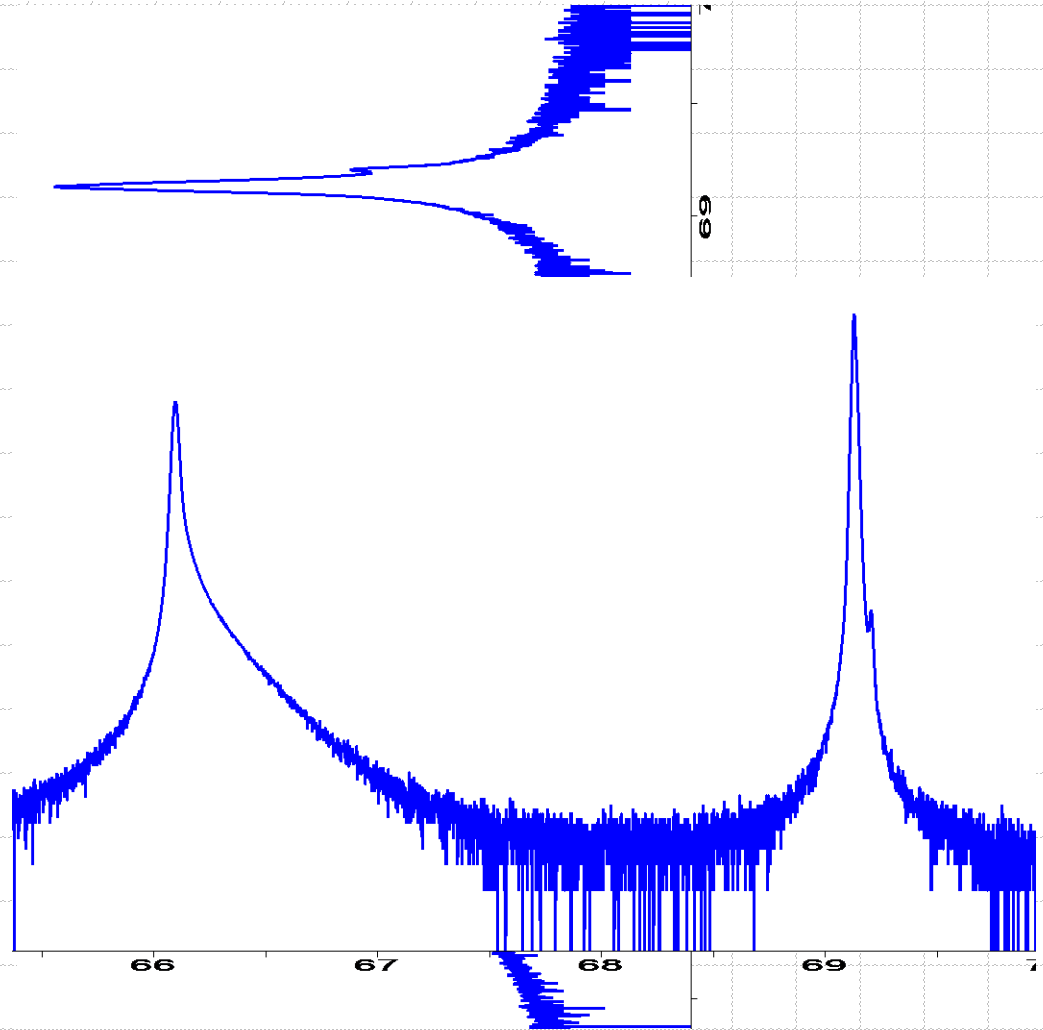
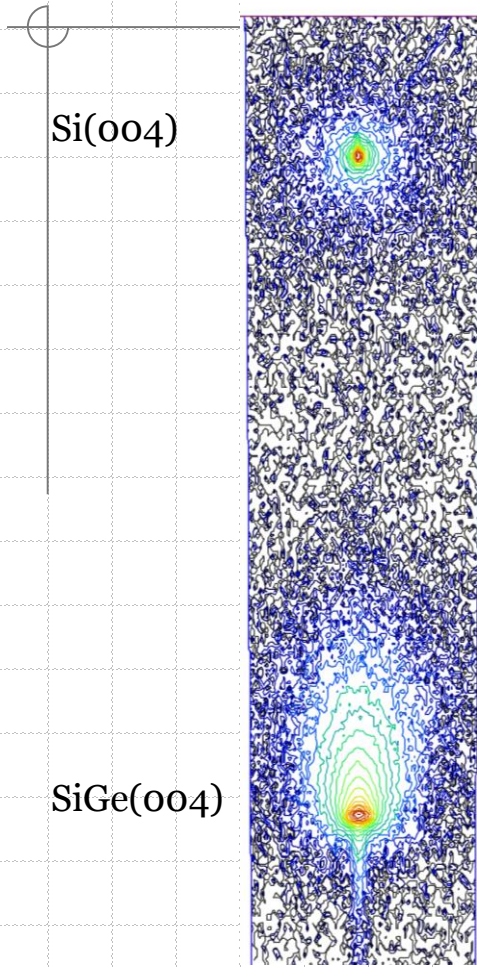
013106c_TA.xrdml

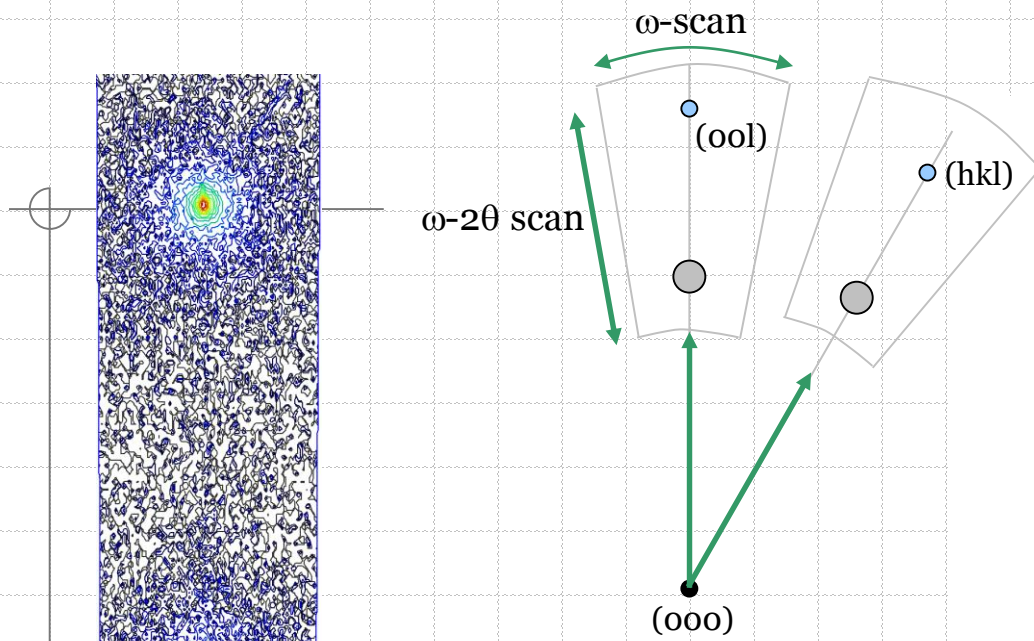


Shape of the RLP might provide much more information

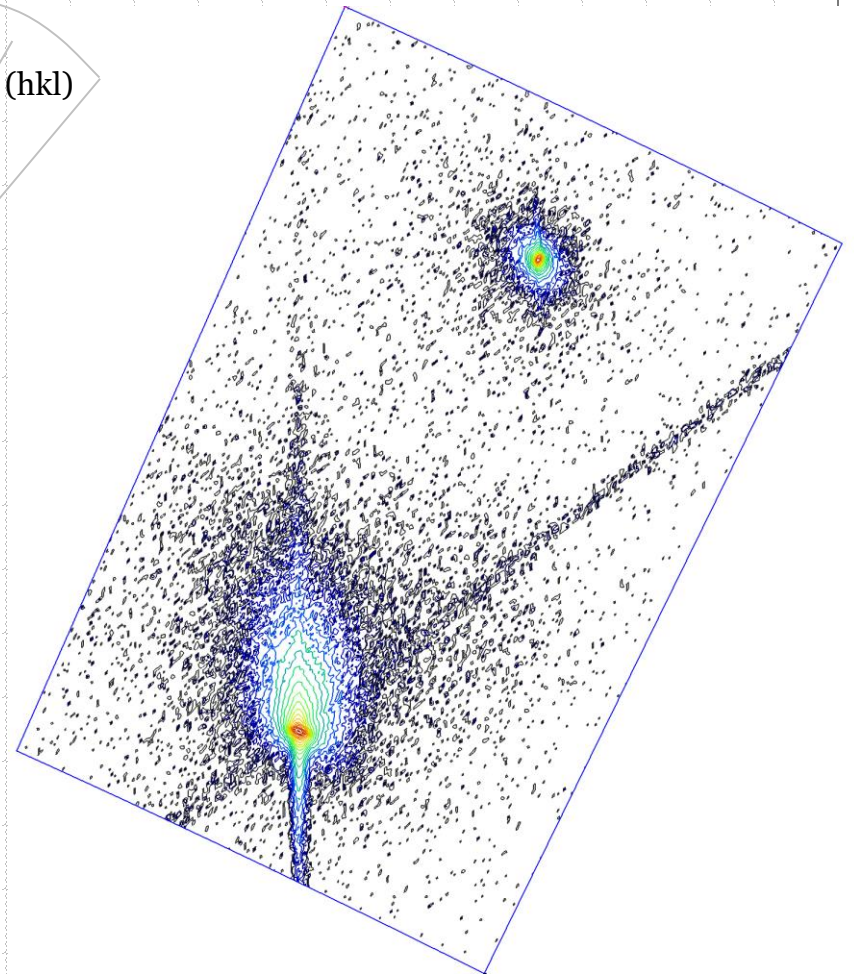
Relaxed SiGe on Si(001)

(004) RLM



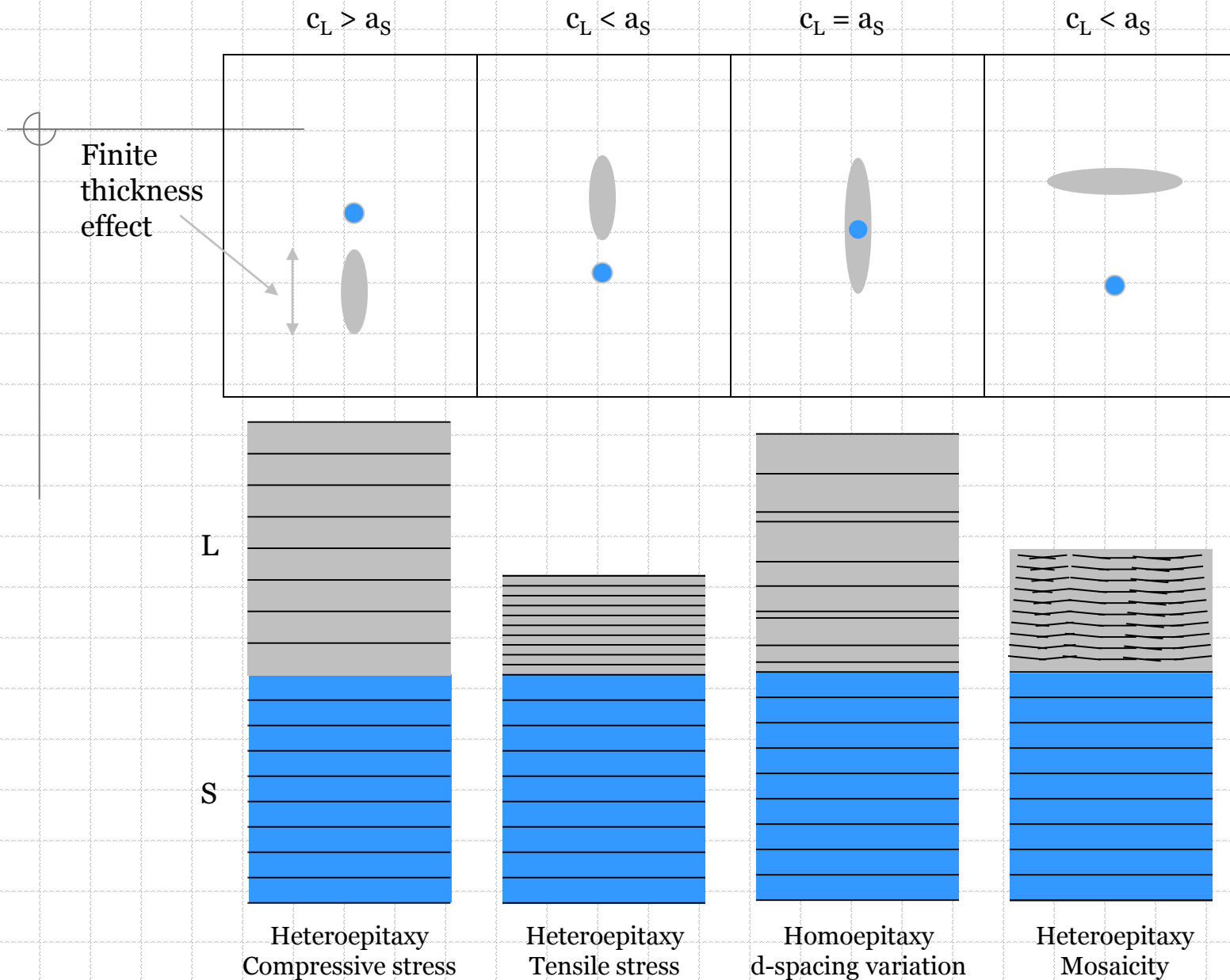


(004)



(113)

Real RLP shapes



004

Omega 33.00650
2Theta 66.01310

Phi 0.00
Psi 0.00

X 0.00
Y 0.00

3683ssl.xrdml

counts/s
10M

1M

100K

10K

1K

100

10

61

62

63

64

65

66

67

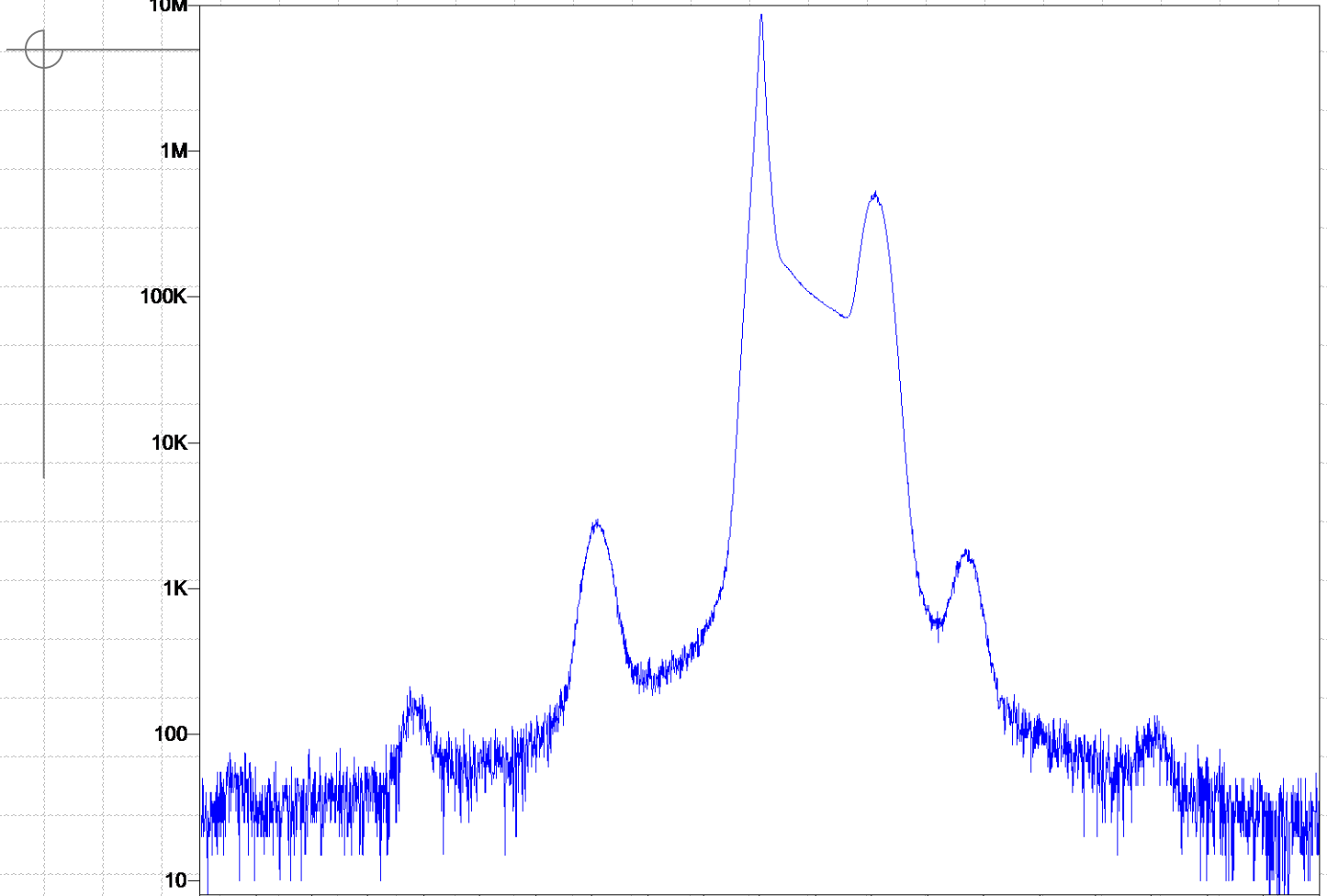
68

69

70

71

2Theta/Omega (°)



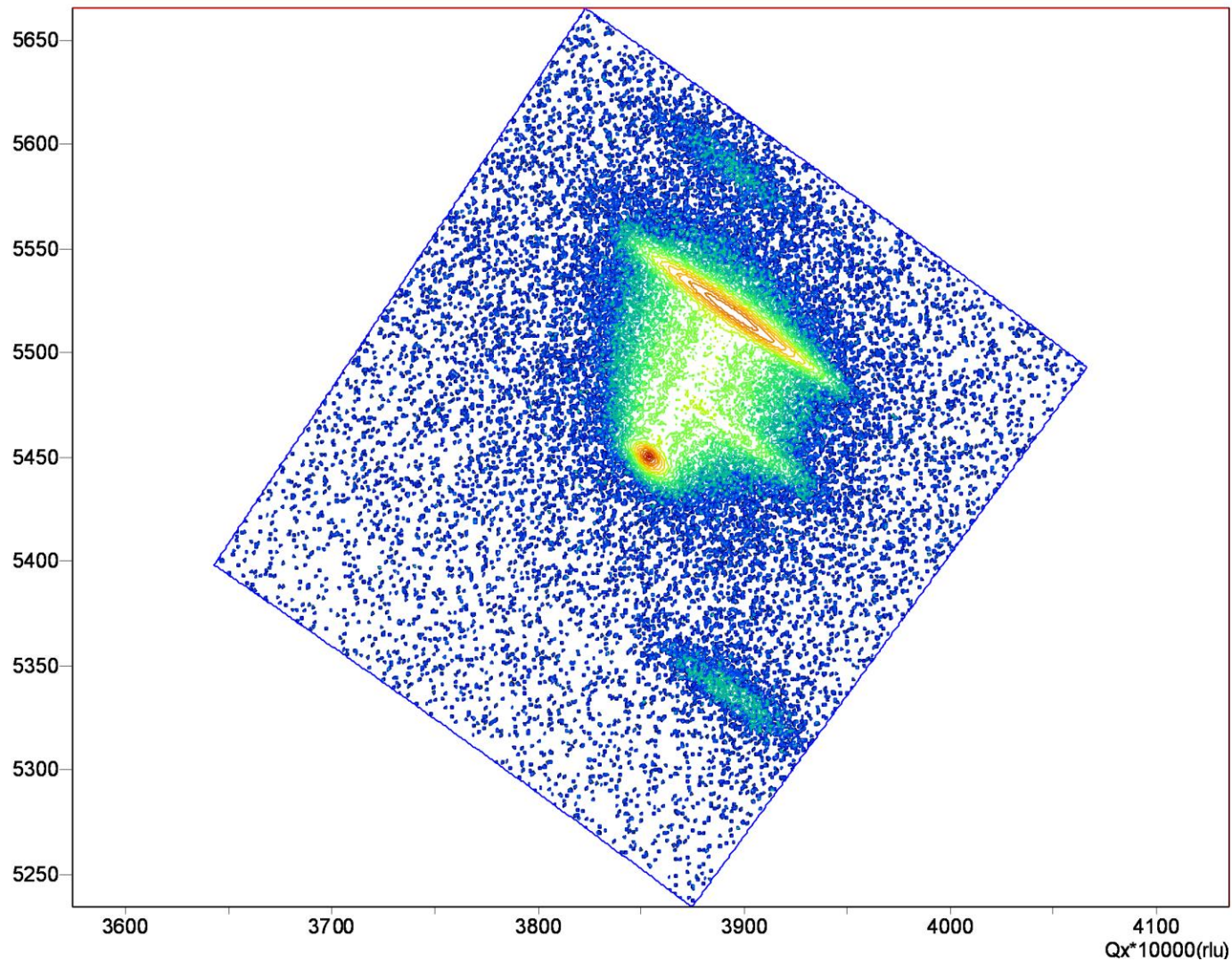
Omega 6.61060
2Theta 83.75000

Phi 0.00
Psi 0.00

X 0.00
Y 13.00
Z 9.110

SLAC_671.xrdml

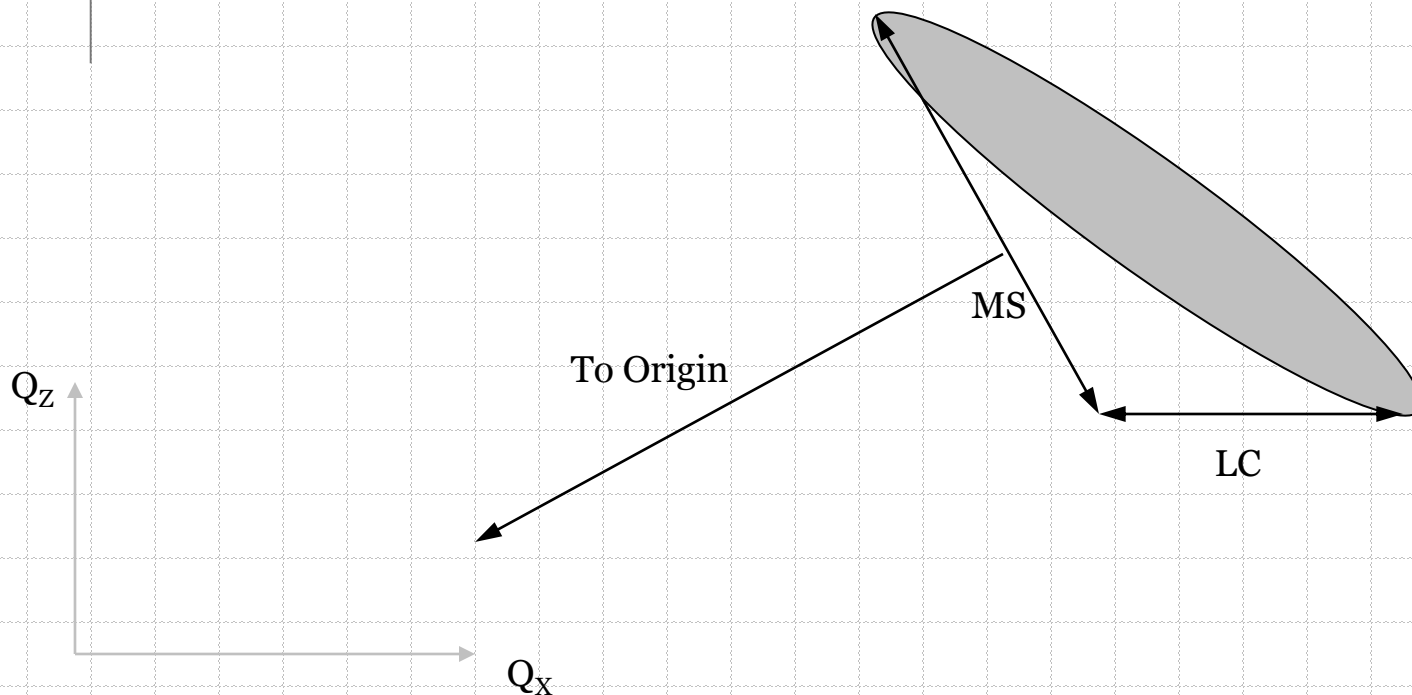
Qy*10000(rlu)



Mosaic Spread and Lateral Correlation Length

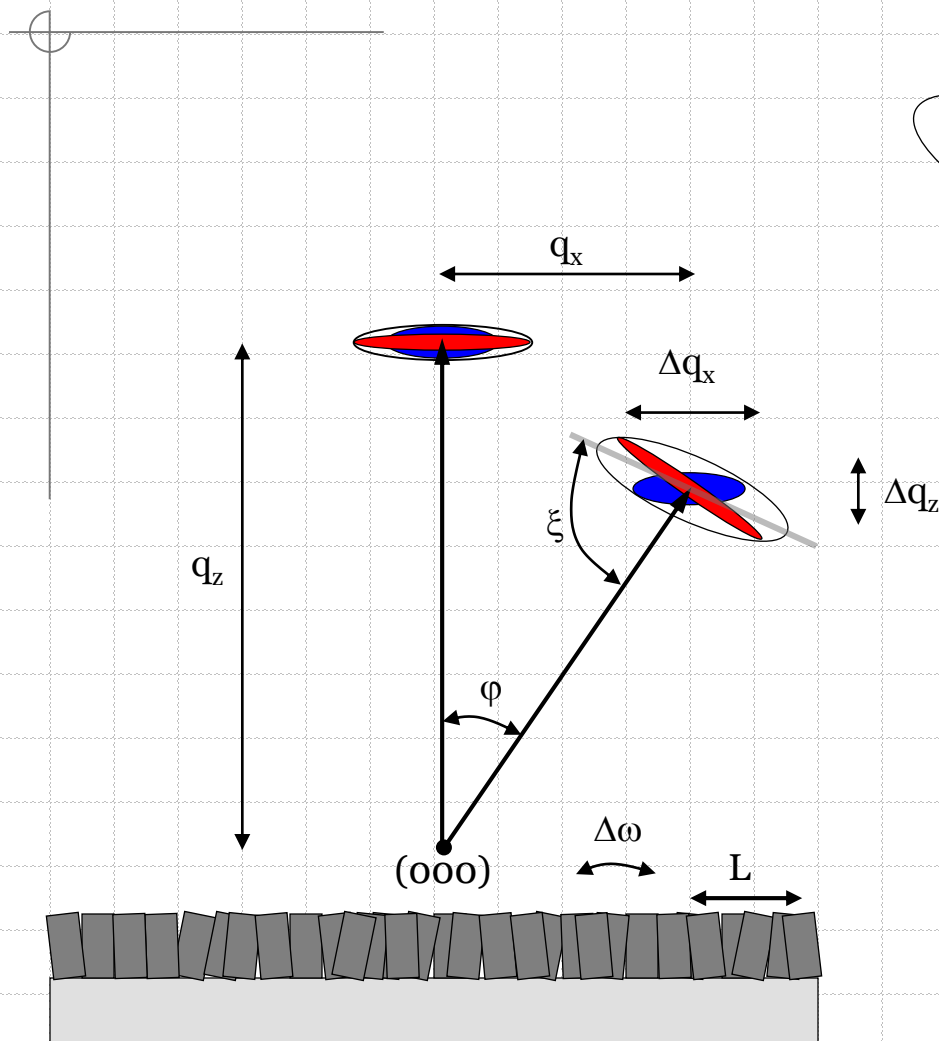
The mosaic spread of the layer is calculated from the angle that the layer peak subtends at the origin of reciprocal space measured perpendicular to the reflecting plane normal.

The lateral correlation length of the layer is calculated from the reciprocal of the FWHM of the peak measured parallel to the interface.



Mosaic Spread and Lateral Correlation Length

The Mosaic Spread and Lateral Correlation Length functionality derives information from the shape of a layer peak in a diffraction space map recorded using an asymmetrical reflection



$$L_3 = \sqrt{\Delta q_x^2 + \Delta q_z^2}$$

and

$$\varphi = \frac{1}{\tan\left(\frac{q_x}{q_z}\right)}$$

$$\xi = \frac{1}{\tan\left(\frac{\Delta q_x}{\Delta q_z}\right)}$$

$$\frac{L_1}{L_2} = -\frac{\cos \xi}{\cos(\varphi + \xi)}$$

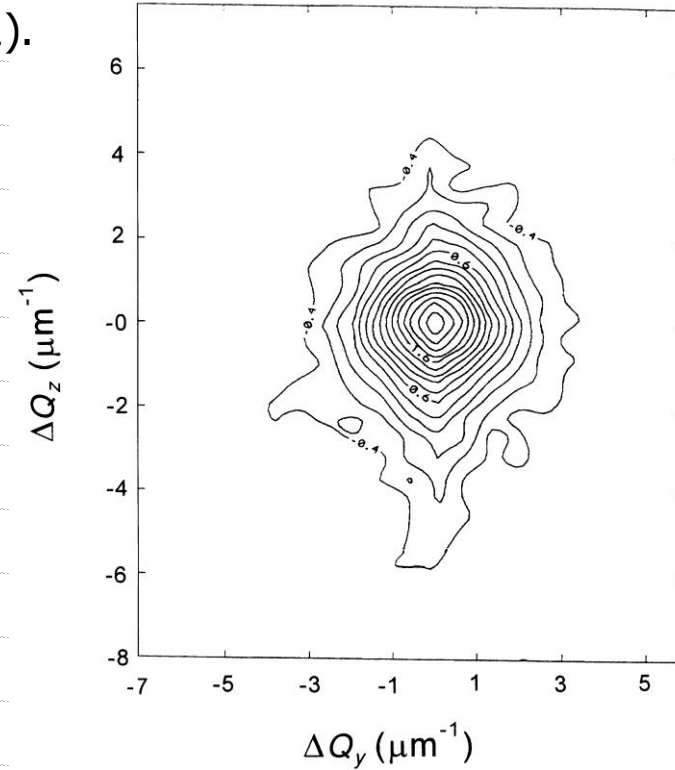
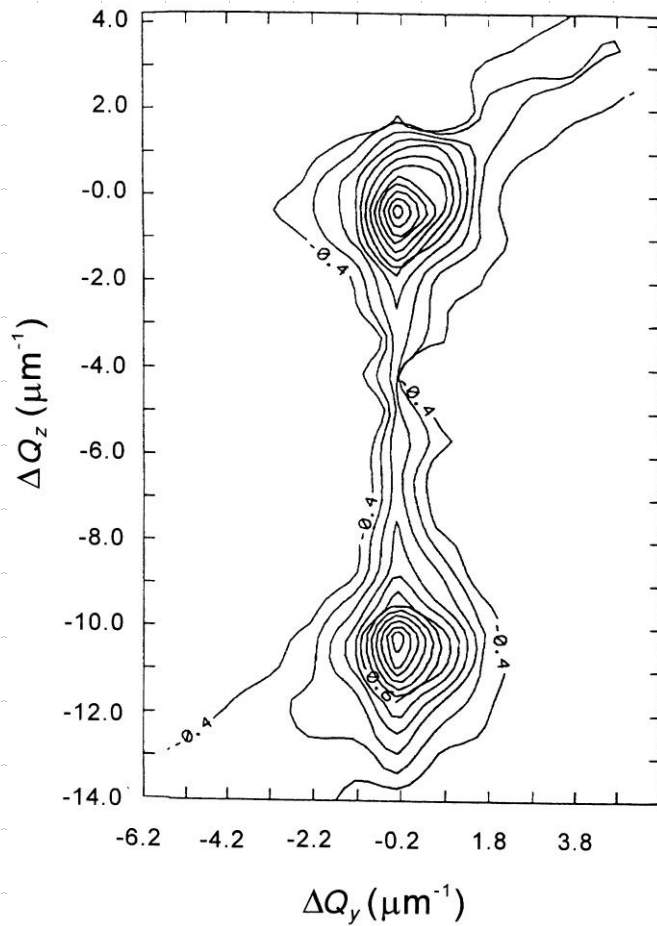
$$\frac{L_3}{L_2} = -\frac{\sin \varphi}{\cos \xi}$$

$$\text{Lateral correlation length} = \frac{1}{L_1}$$

$$\text{Microscopic tilt} = \frac{L_2}{\sqrt{q_x^2 + q_z^2}}$$

Applications of RLM

Thin epitaxial GaAs film on GaAs(001).
Film has more As.



RLM after annealing

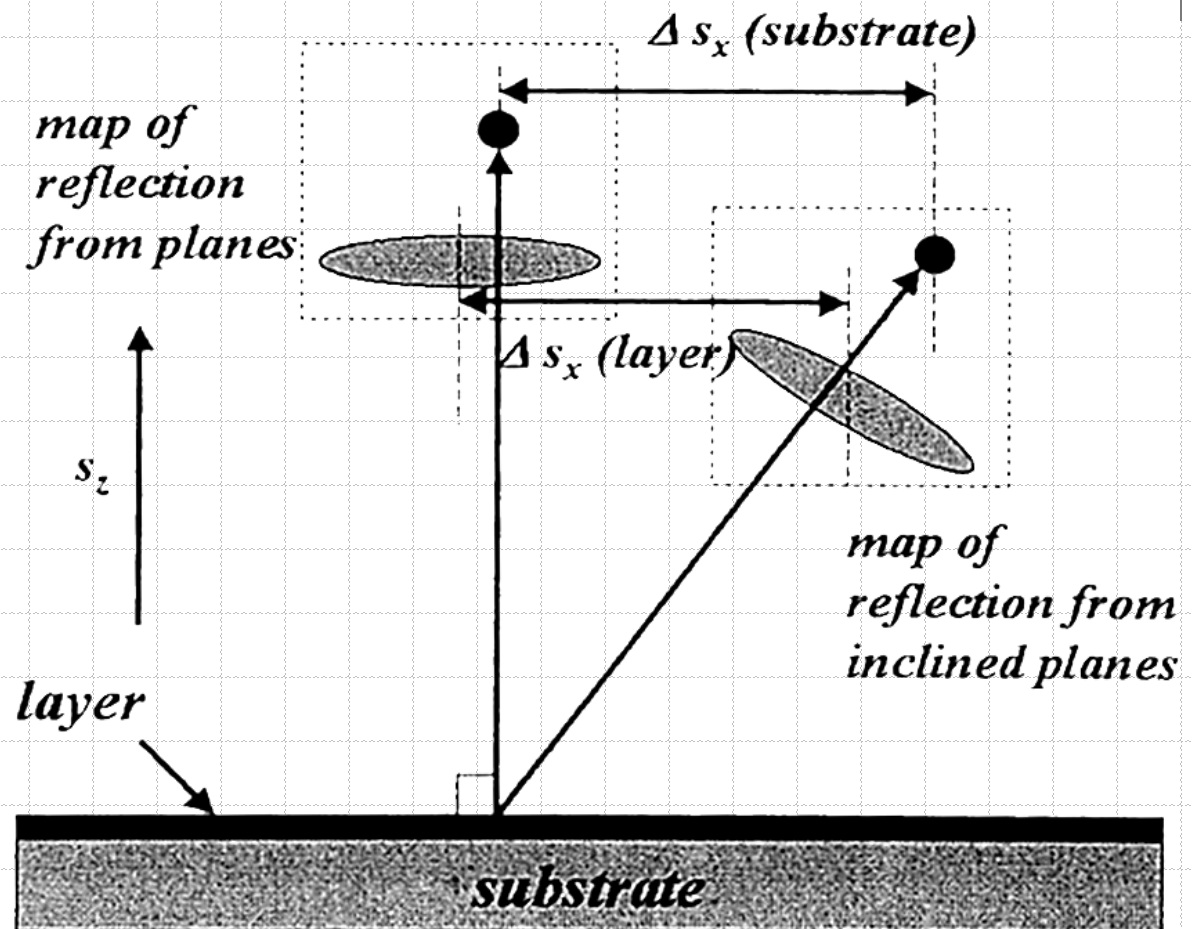
Strain in Partially Relaxed Layers

- ◆ A schematic of the measurements to be extracted from two RLM's to determine the relaxation of a layer on a substrate.

$$s_x = \frac{q_x}{2\pi} = \frac{1}{\lambda} \{ \cos \omega - \cos(2\theta - \omega) \}$$

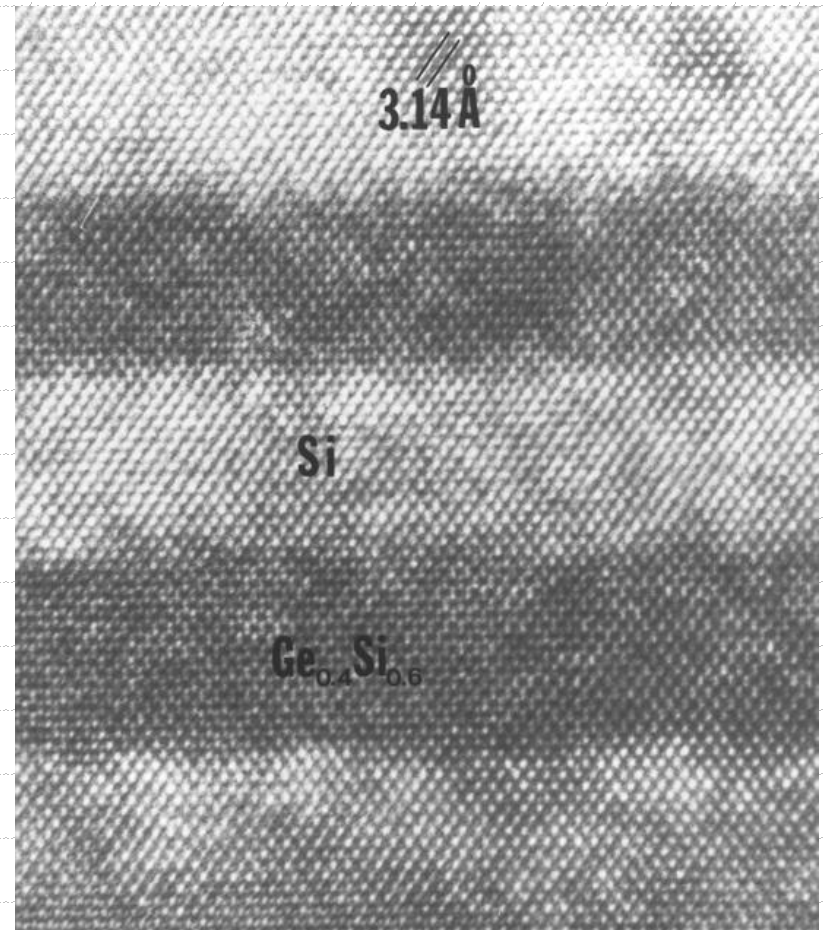
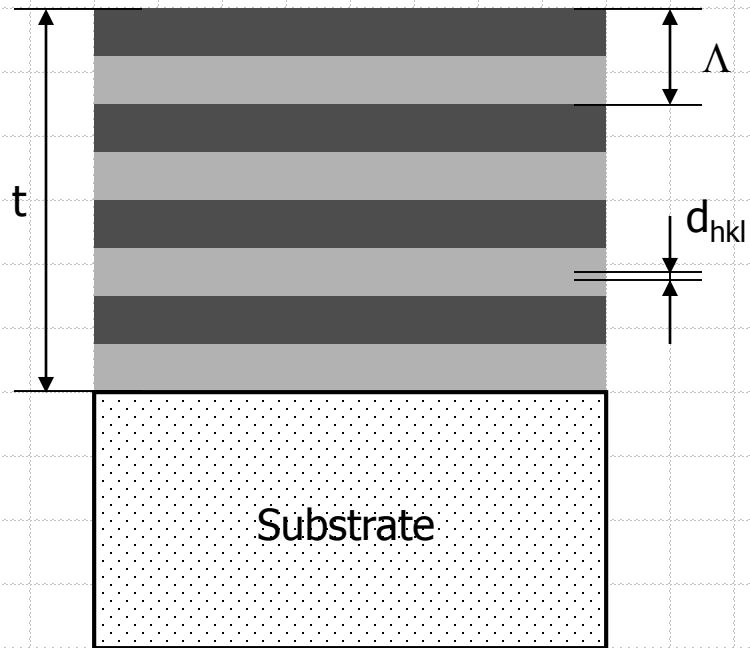
$$s_z = \frac{q_z}{2\pi} = \frac{1}{\lambda} \{ \sin \omega - \sin(2\theta - \omega) \}$$

$$q = \frac{4\pi \sin \theta}{\lambda}$$



Superlattices and Multilayers

- ◆ Transmission electron micrograph depicts one of the earliest multilayer, GeSi / Si "superlattices." The dots are the actual images of individual columns of atoms.

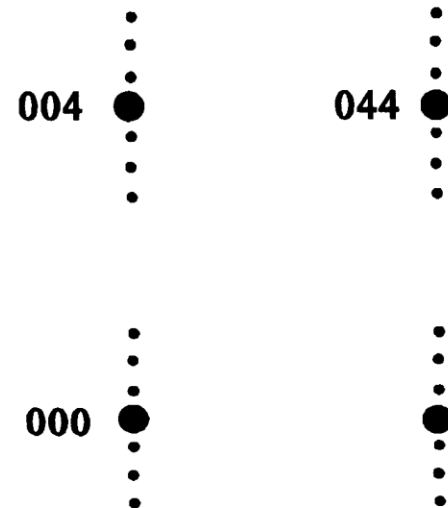
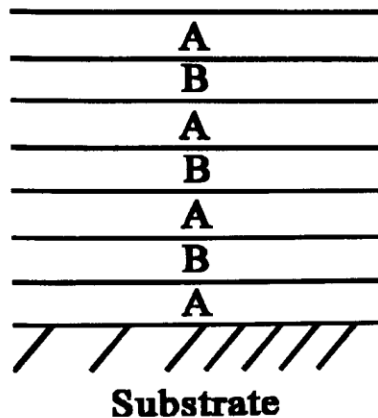
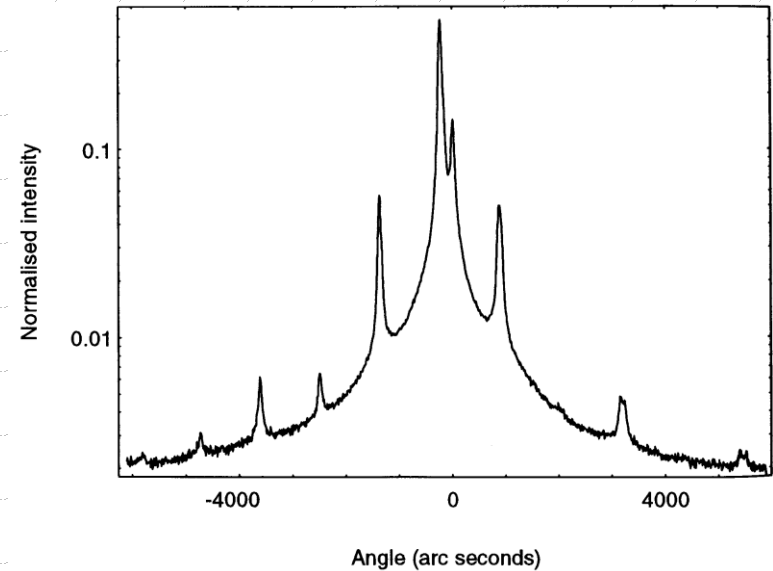


Superlattices and Multilayers

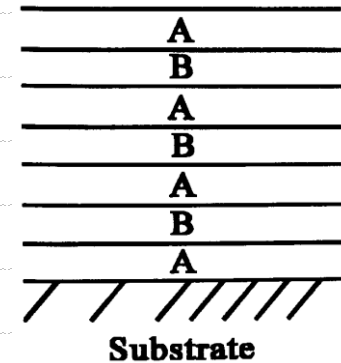
- ◆ General characteristics of large repeat superlattices
 - The spatial period of the structure
 - The thickness of the repeating unit
 - The composition of the layers
 - The dispersion in the repeating period
 - The interface roughness
 - The interface grading

Superlattices and Multilayers

- ◆ Double-axis rocking curve from an AlGaAs/GaAs superlattice.
 - Cu $K\alpha$ radiation, 004 reflection

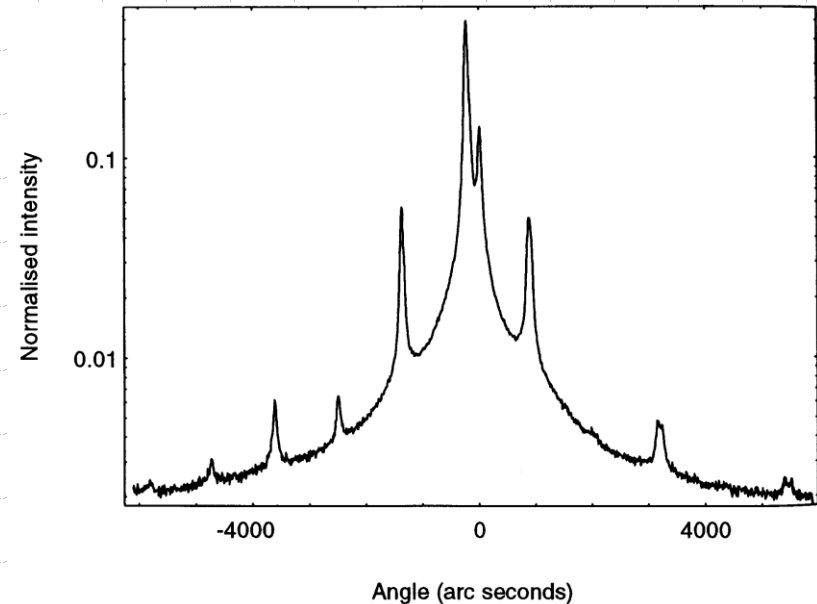


Superlattices and Multilayers



◆ The rocking curve shows the following features:

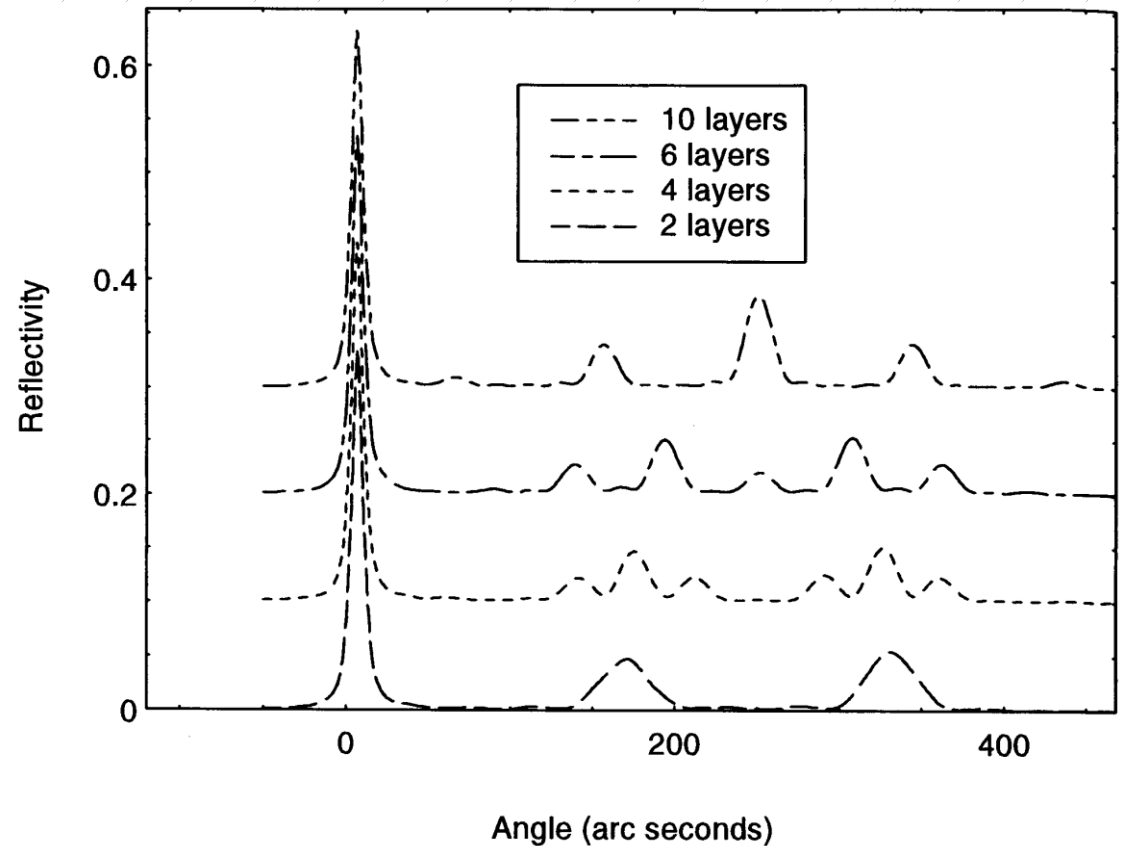
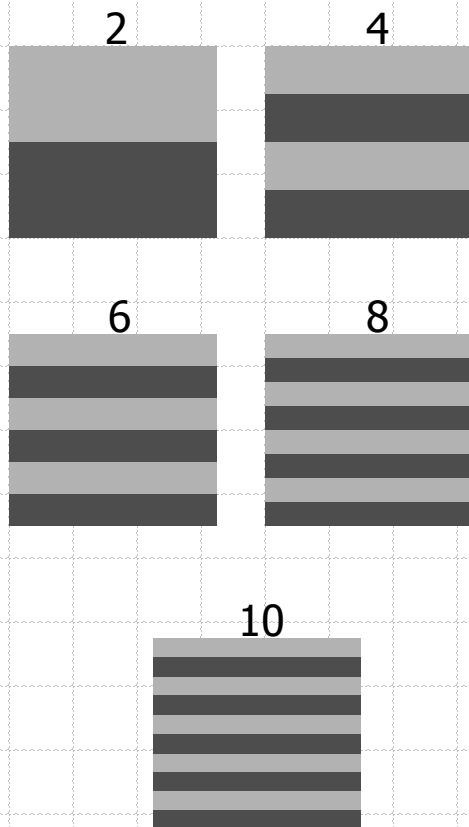
- A substrate peak from the A substrate
- A peak caused by the addition of Bragg reflections from the A and B components of the MQW. This is zero-order or average mismatch peak, from which the average composition of the A+B layers may be obtained by differentiation of Bragg's law.
- A set of subsidiary "satellite" peaks symmetrically surrounding the zero-order peak, with spacing determined by the periodicity (total thickness of the repeating layers) of the MQW.



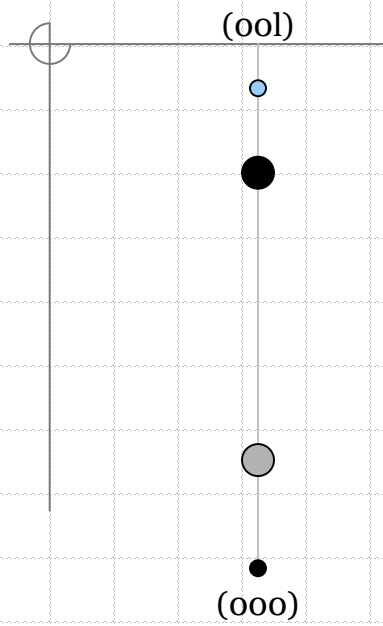
XRD pattern from multiple quantum well (MQW) with substrate A (GaAs) and stack of AB layers where B is alloy (e.g. $\text{Ga}_{1-x}\text{Al}_x\text{As}$).

Superlattices and Multilayers

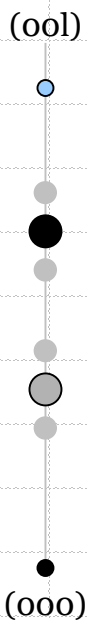
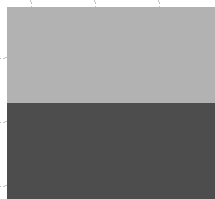
- ◆ Simulated rocking curves from an epilayer of total thickness $1\mu\text{m}$, subdivided into 2, 4, 6 and 10 layers of alternate composition.



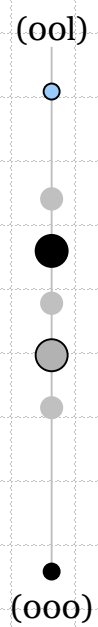
Superlattices and Multilayers



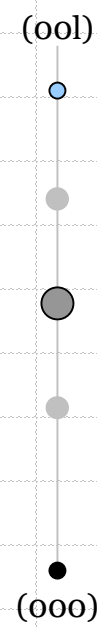
2



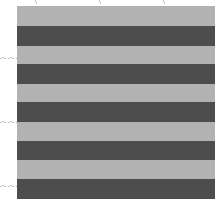
4



6

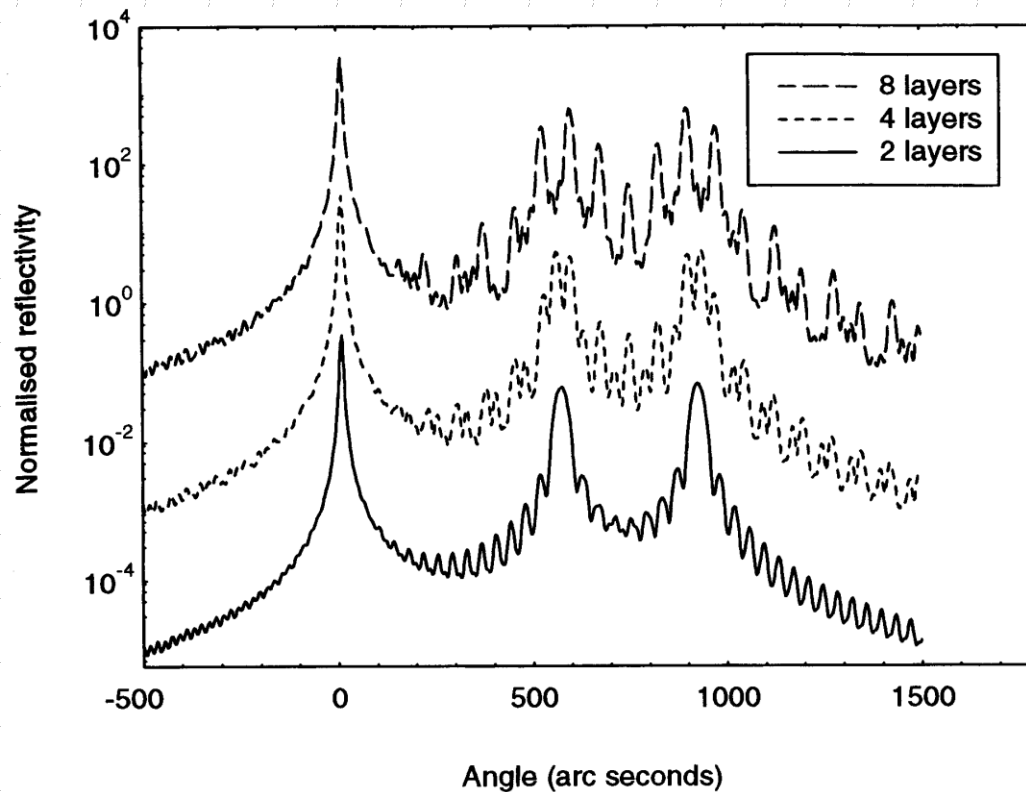


10



Superlattices and Multilayers

- ◆ Simulated rocking curve from sequence of layers of total thickness $1\mu\text{m}$, divided into 2, 4 and 8 repeats of $\text{In}_x\text{Ga}_{1-x}\text{As}$ layers of composition $x = 0.5$ and $x = 0.43$.

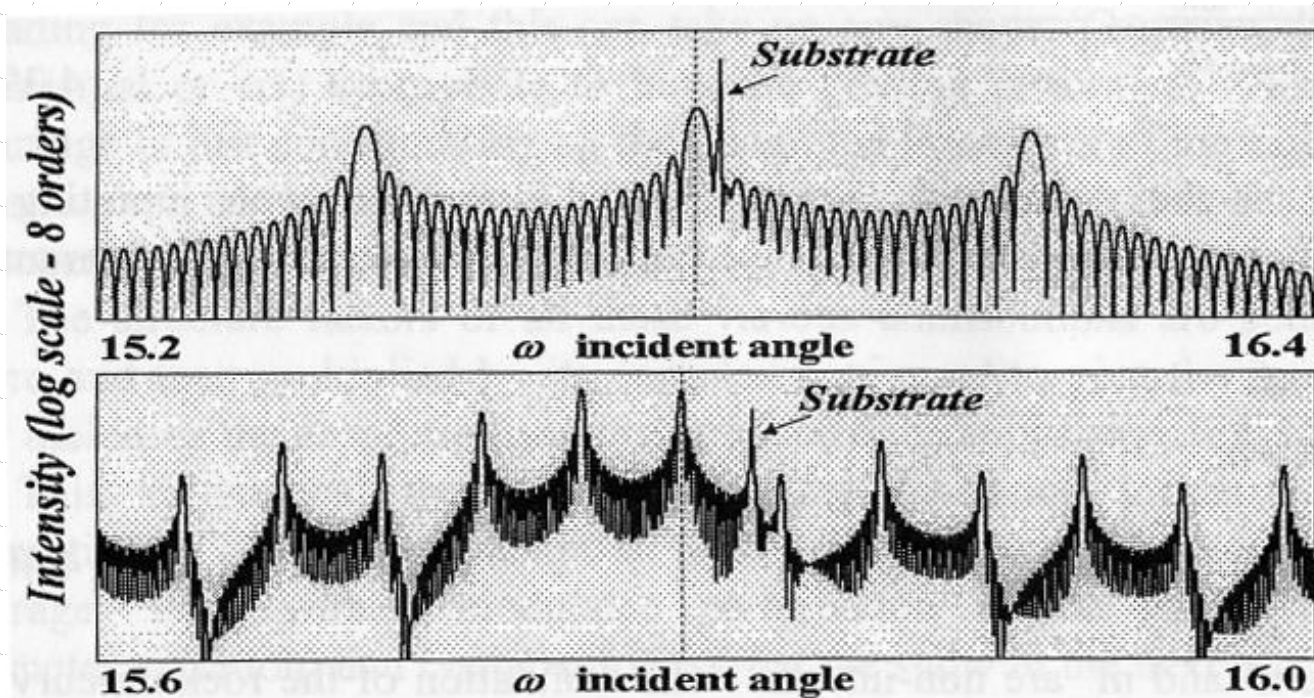


Superlattices and Multilayers

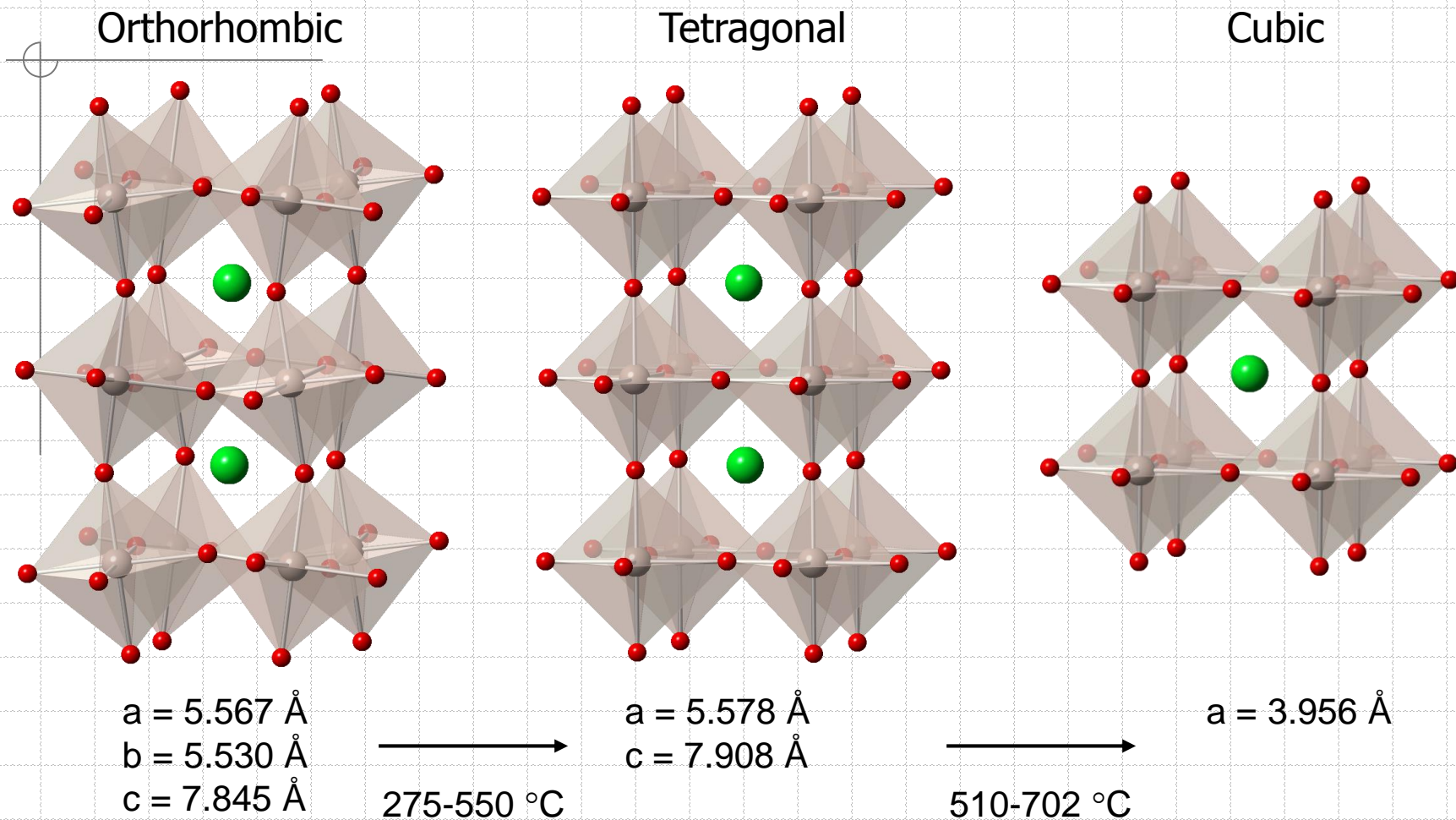
- ◆ The multilayer periodicity is defined as:

$$\Lambda = \frac{(n_i - n_j)\lambda}{2(\sin \omega_i - \sin \omega_j)}$$

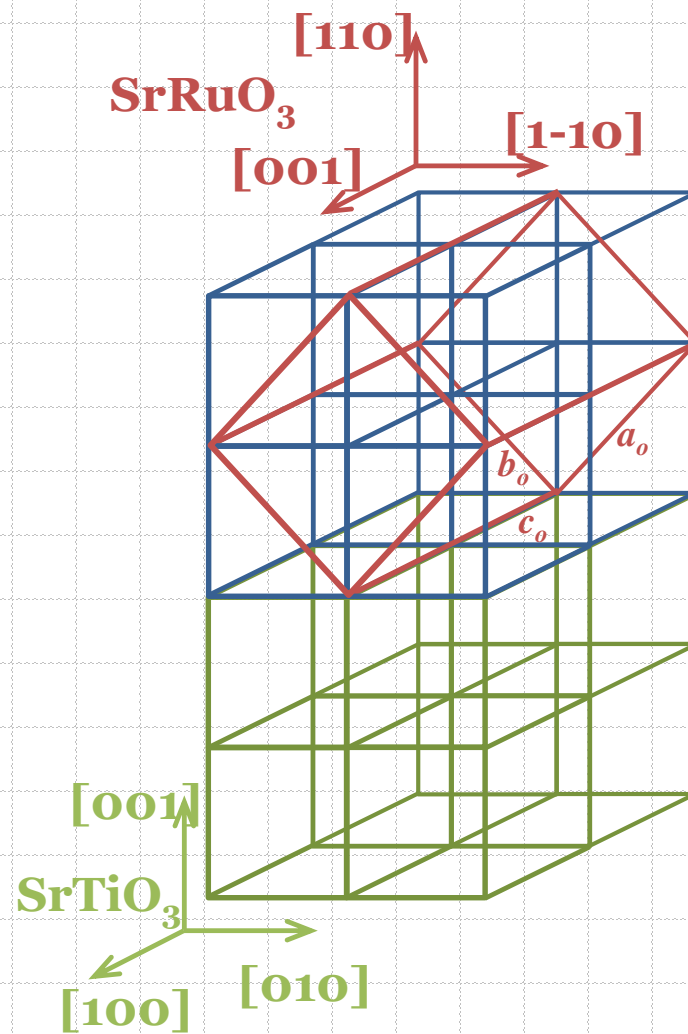
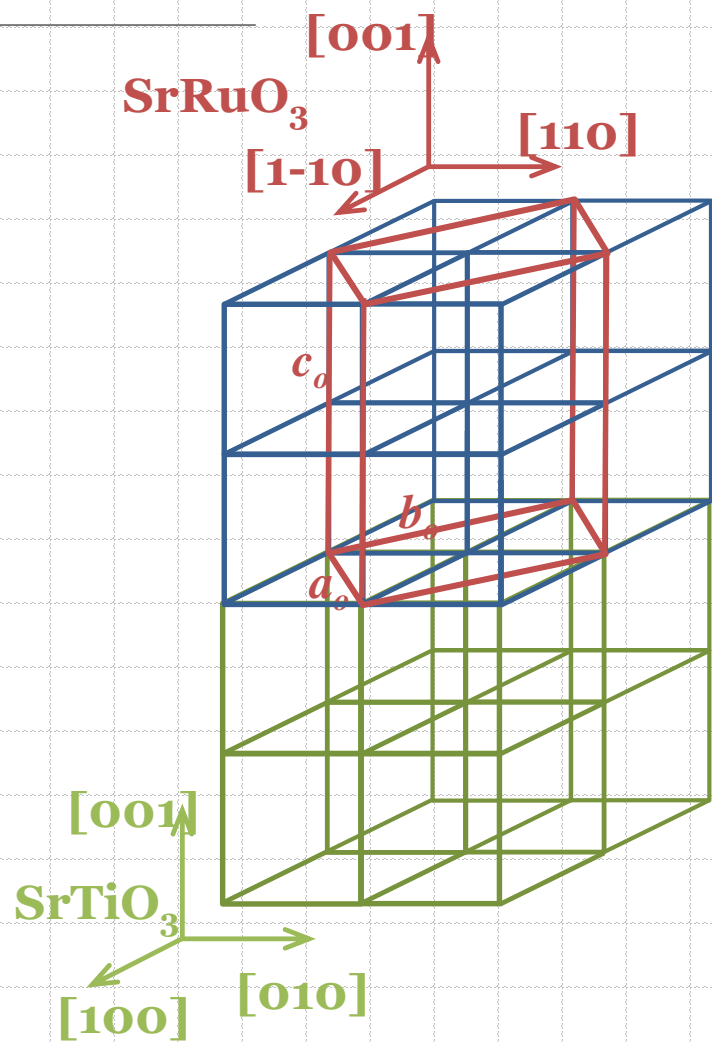
equation defines satellite peak positions

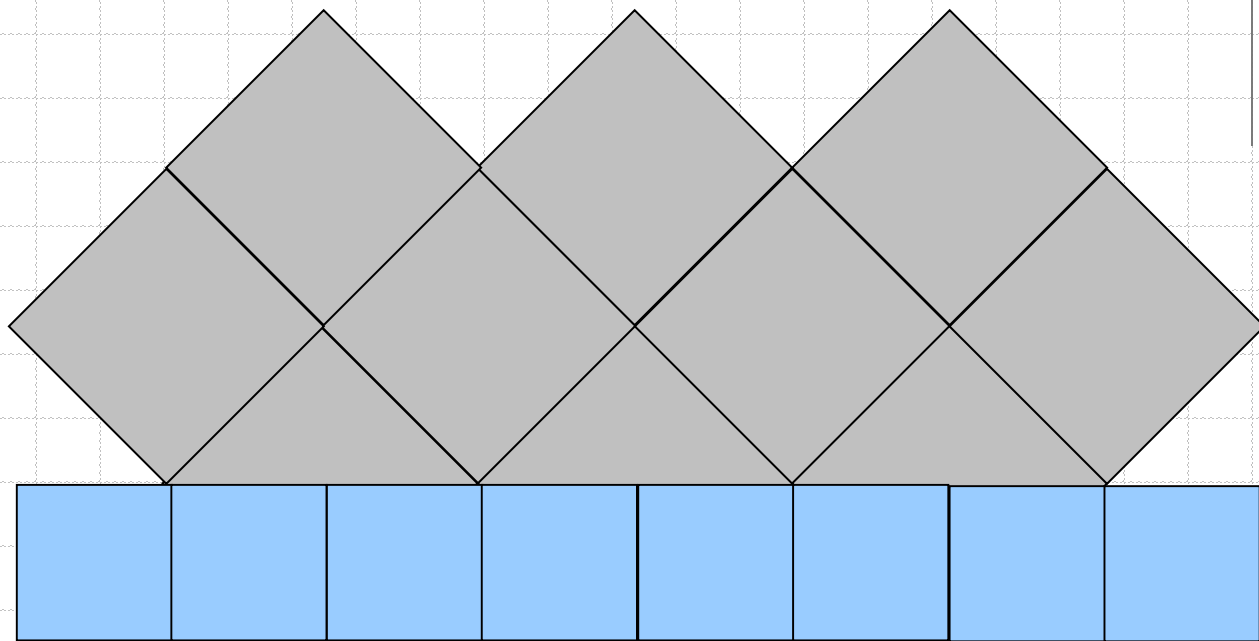
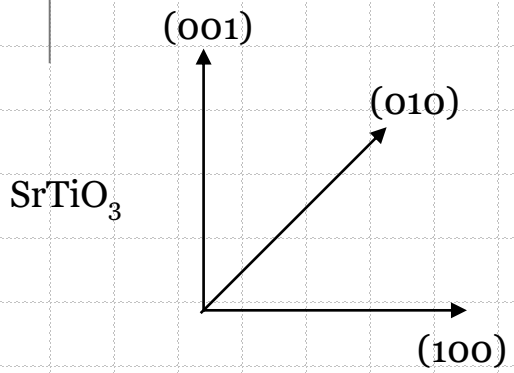
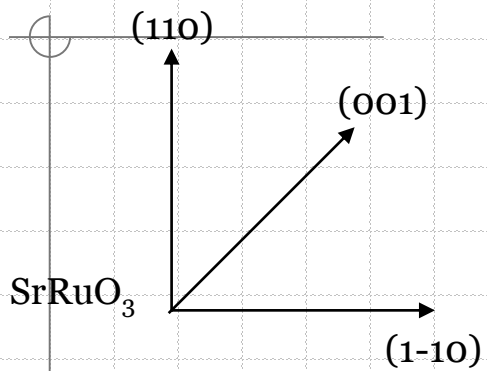


Structure of SrRuO₃

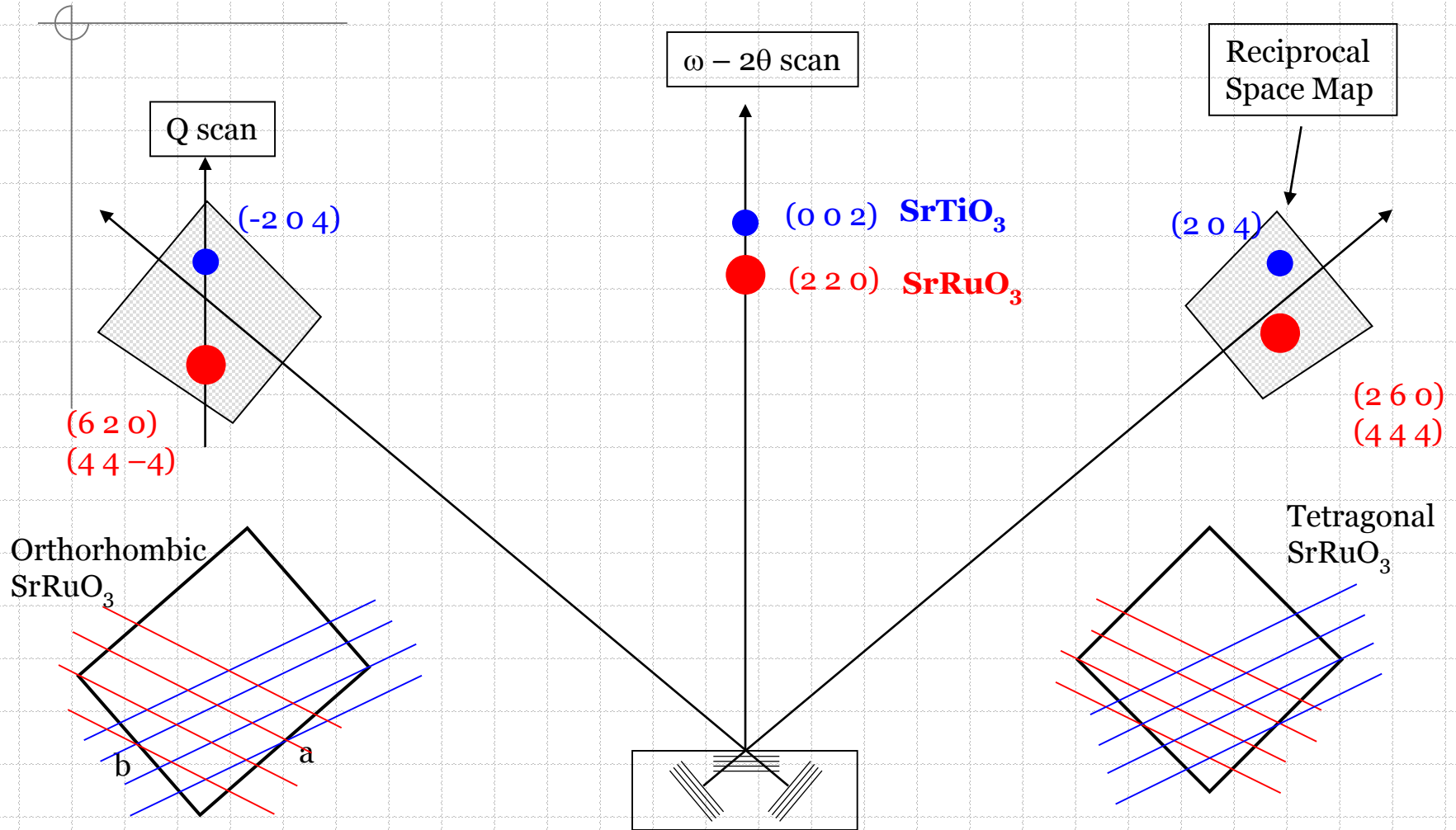


Structure of SrRuO₃



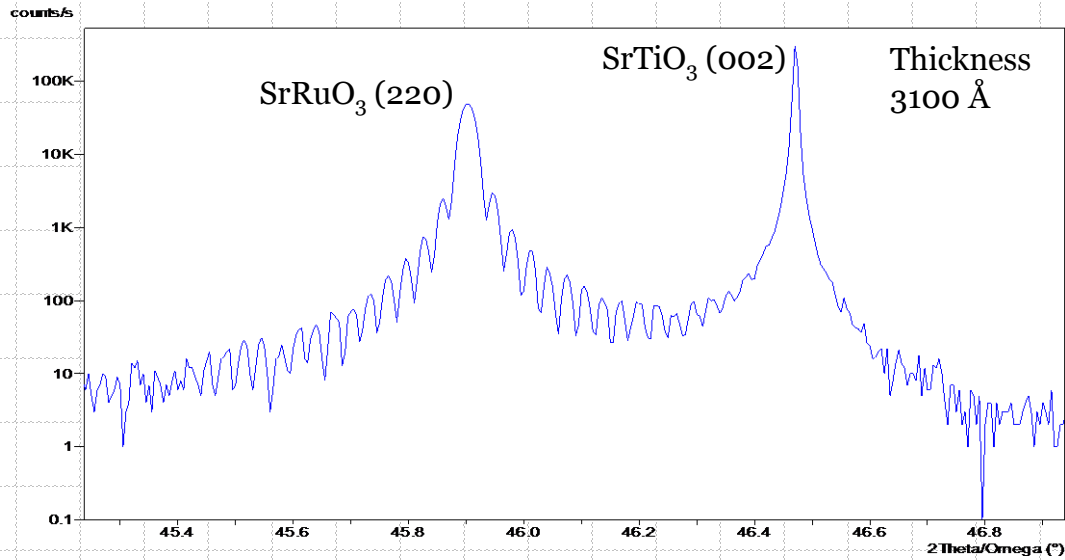
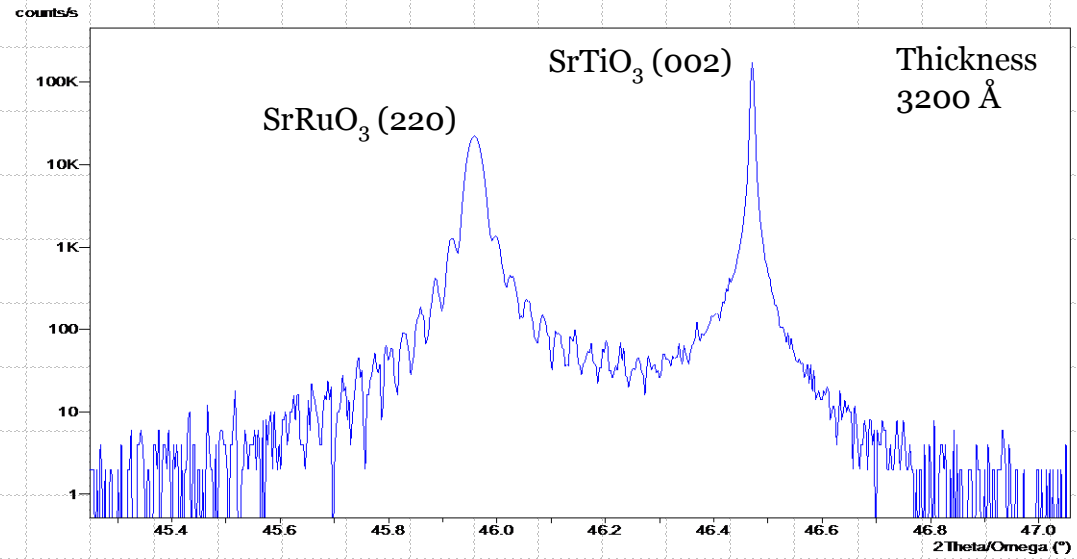


X-ray Diffraction Scan Types



$\omega - 2\theta$ symmetrical scans

Finite size fringes indicate well ordered films



Reciprocal Lattice Map of SrRuO₃ (220) and SrTiO₃ (002)

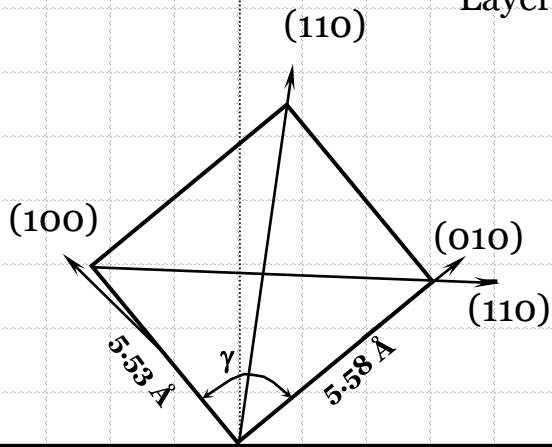
Distorted perovskite structure:
Films are slightly distorted from orthorhombic, $\gamma = 89.1^\circ - 89.4^\circ$

$\omega - 2\theta$ scan

- (0 0 2) SrTiO₃
- (2 2 0) SrRuO₃

Substrate

Layer



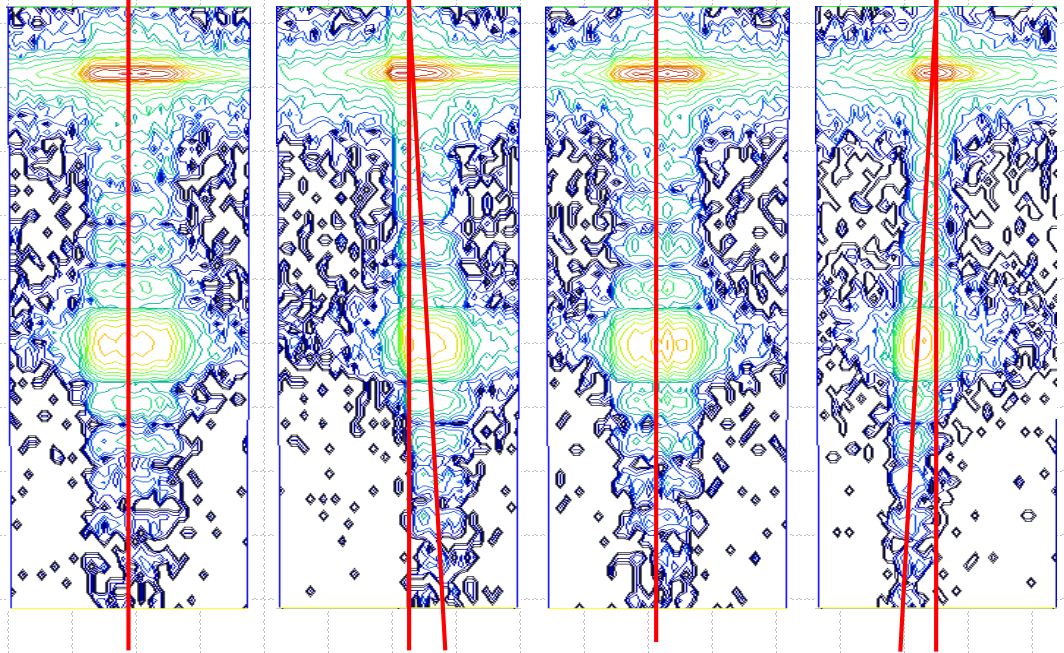
0°

90°

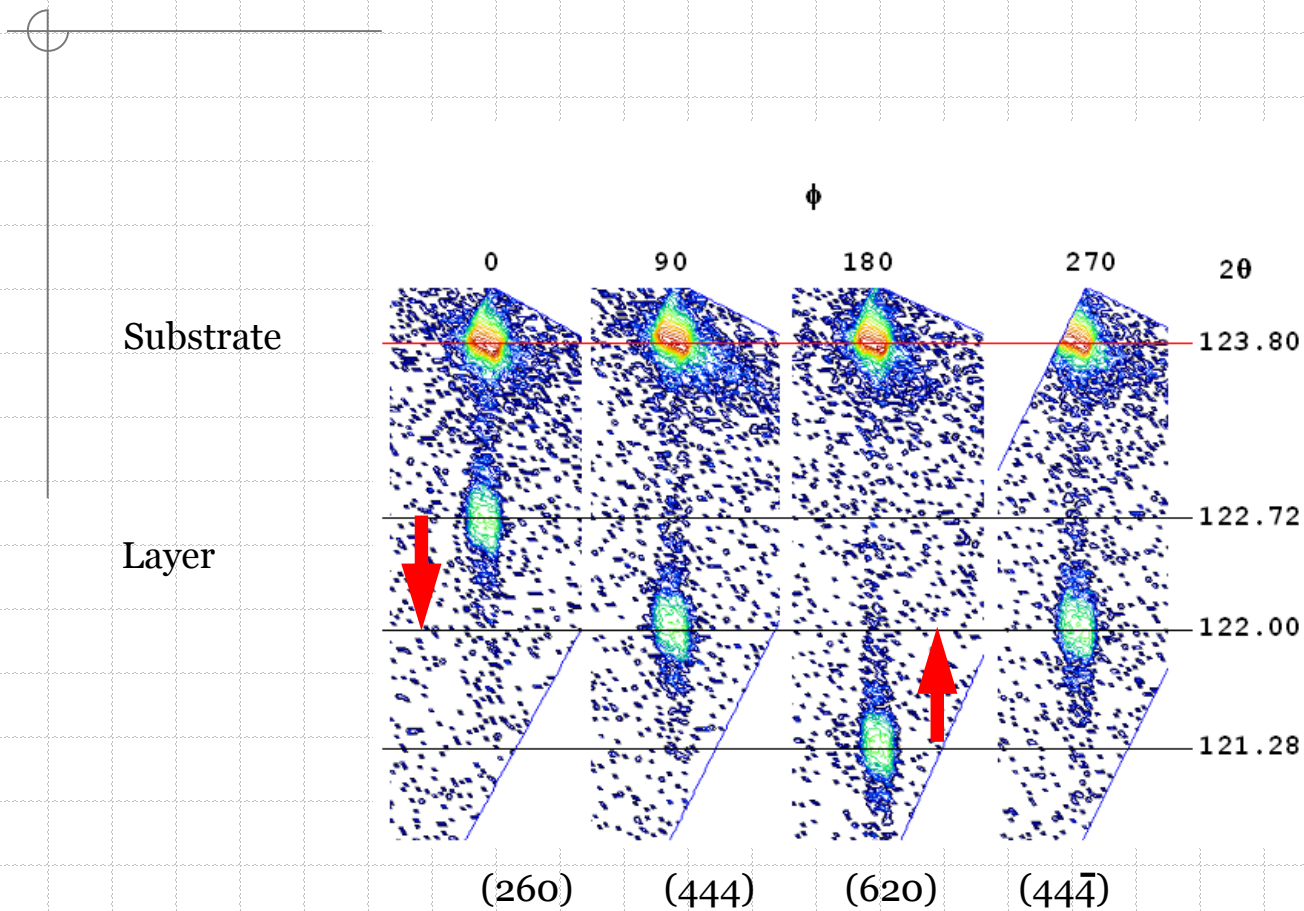
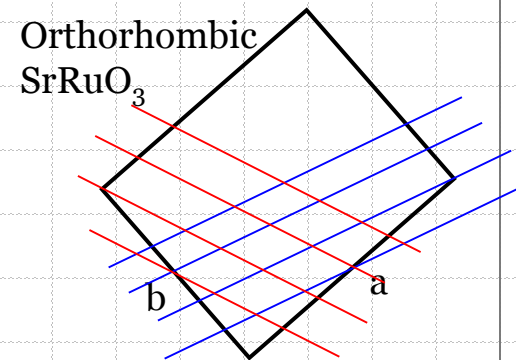
ϕ angle

180°

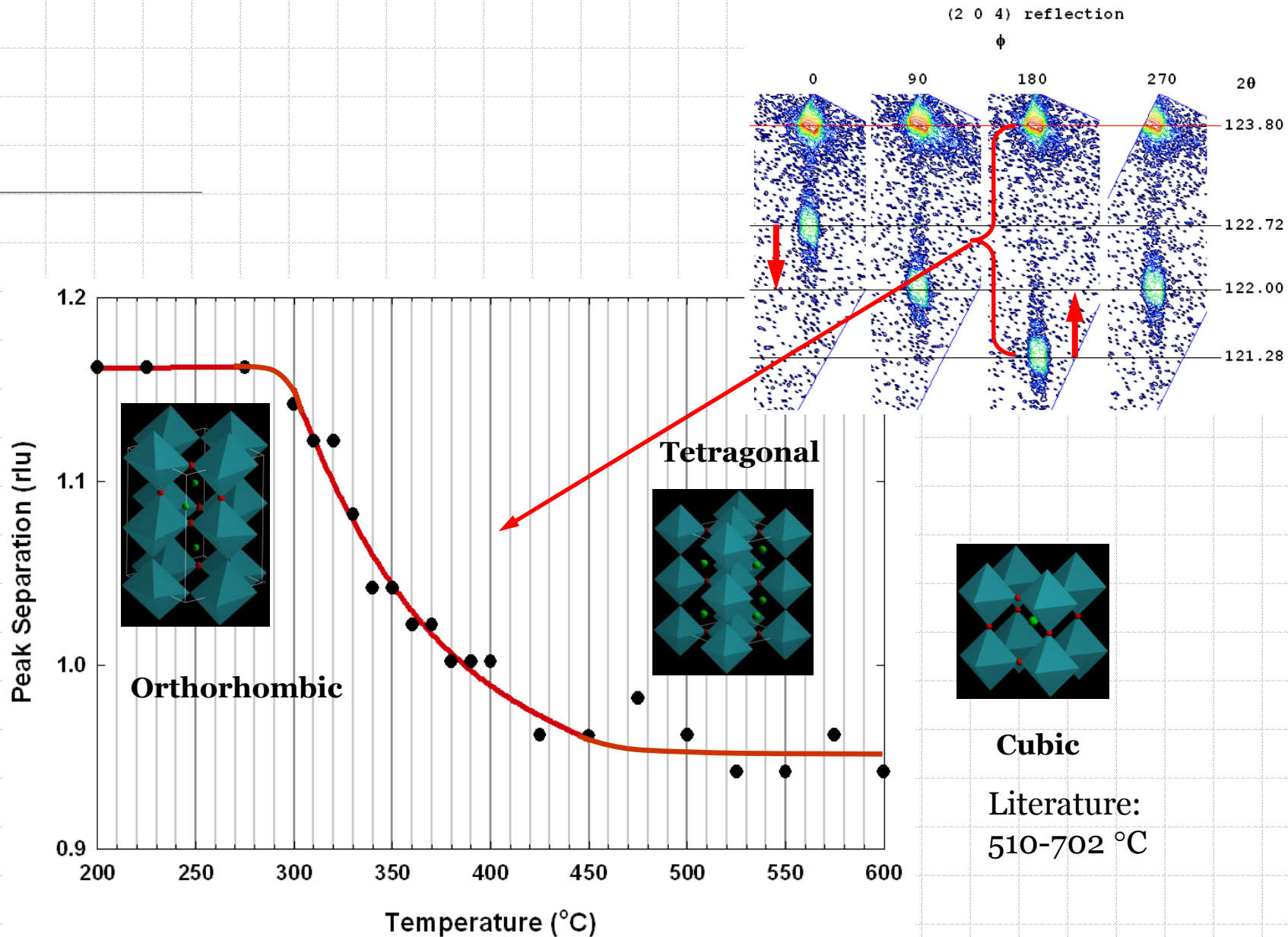
270°



High-Resolution Reciprocal Area Mapping



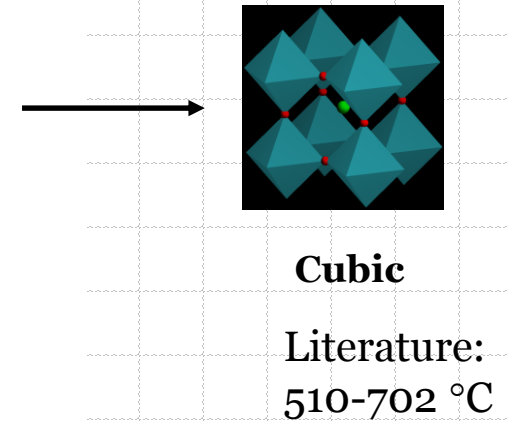
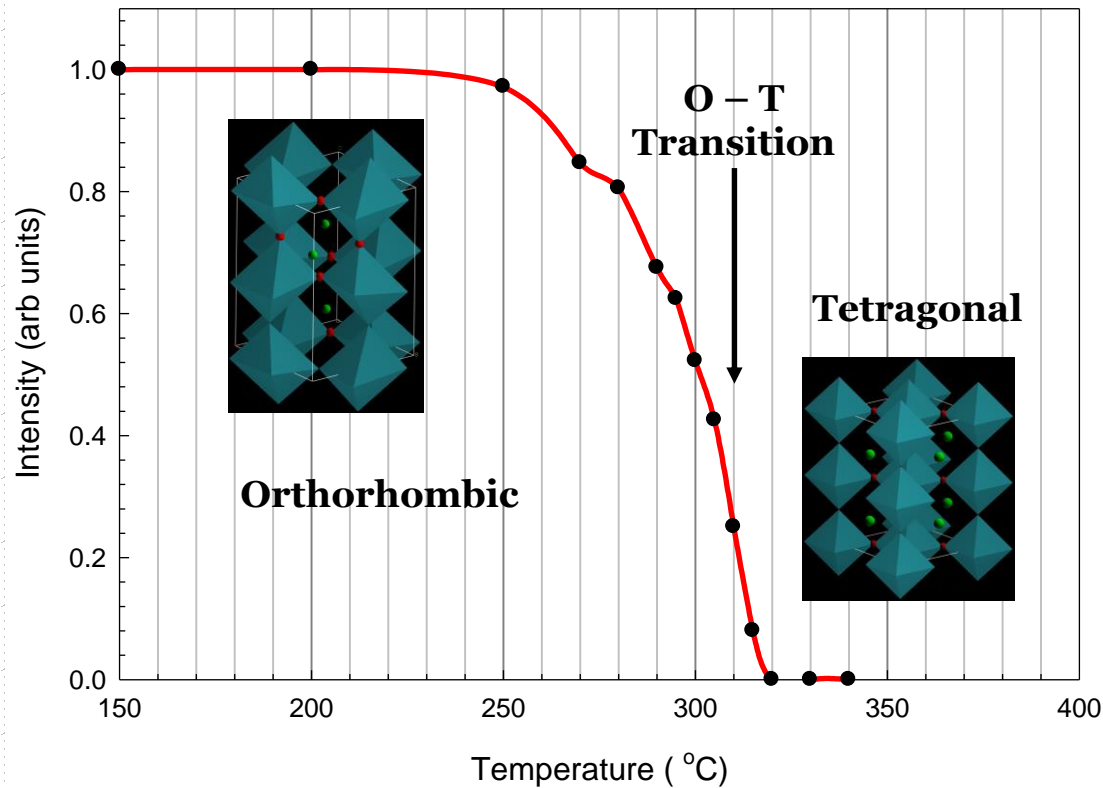
Orthorombic to Tetragonal Transition



Transition Orthorhombic to Tetragonal ~ 350 °C

Structural Transition, (221) reflection

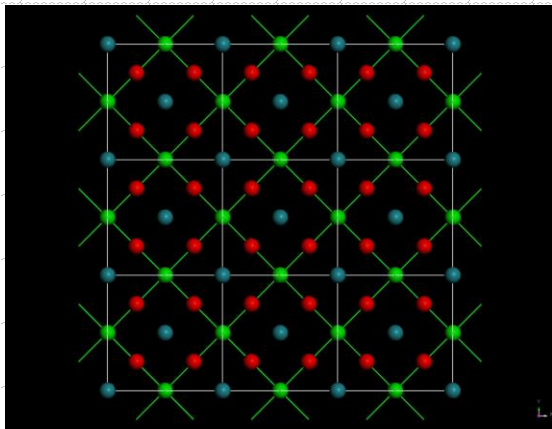
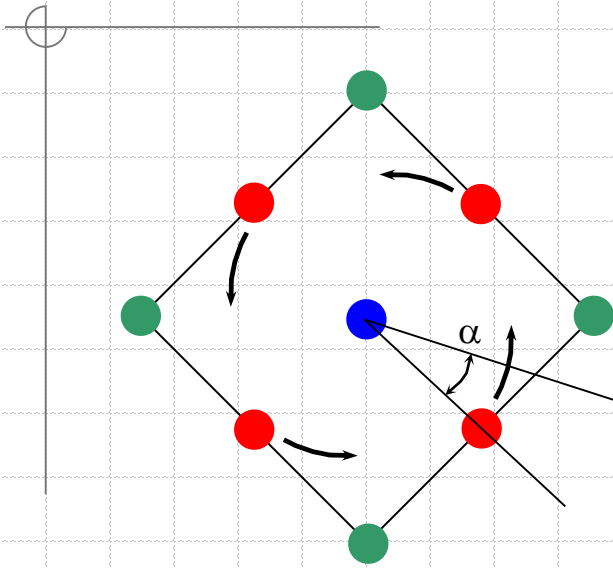
(221) Peak	
Orthorhombic	Present
Tetragonal	Absent



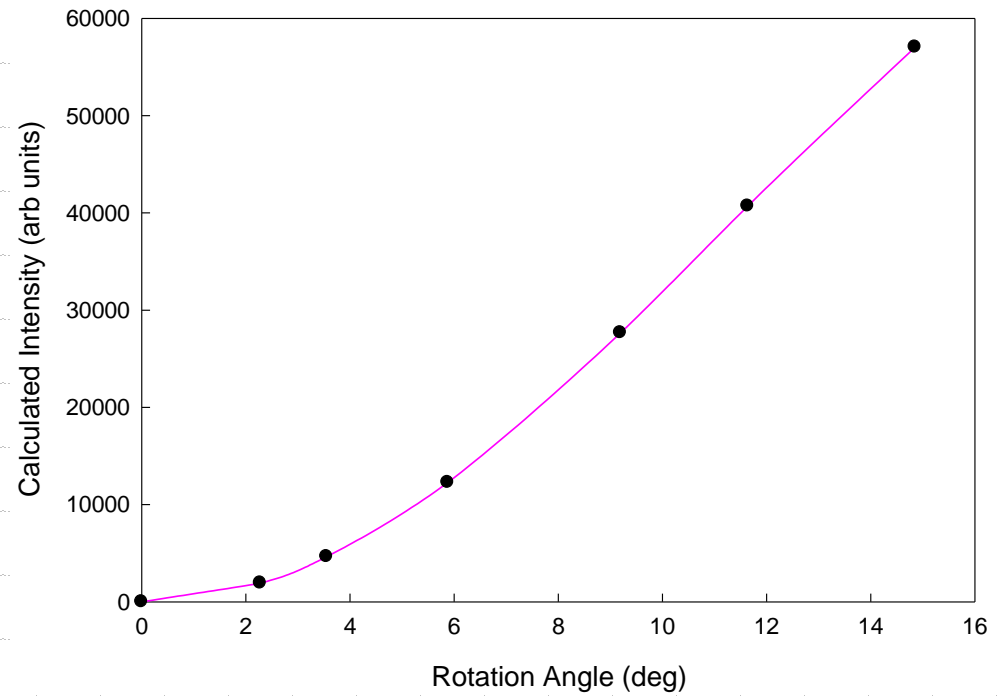
Transition Orthorhombic to Tetragonal ~ 310 °C

Transition Orthorhombic to Tetragonal ~ 310 °C

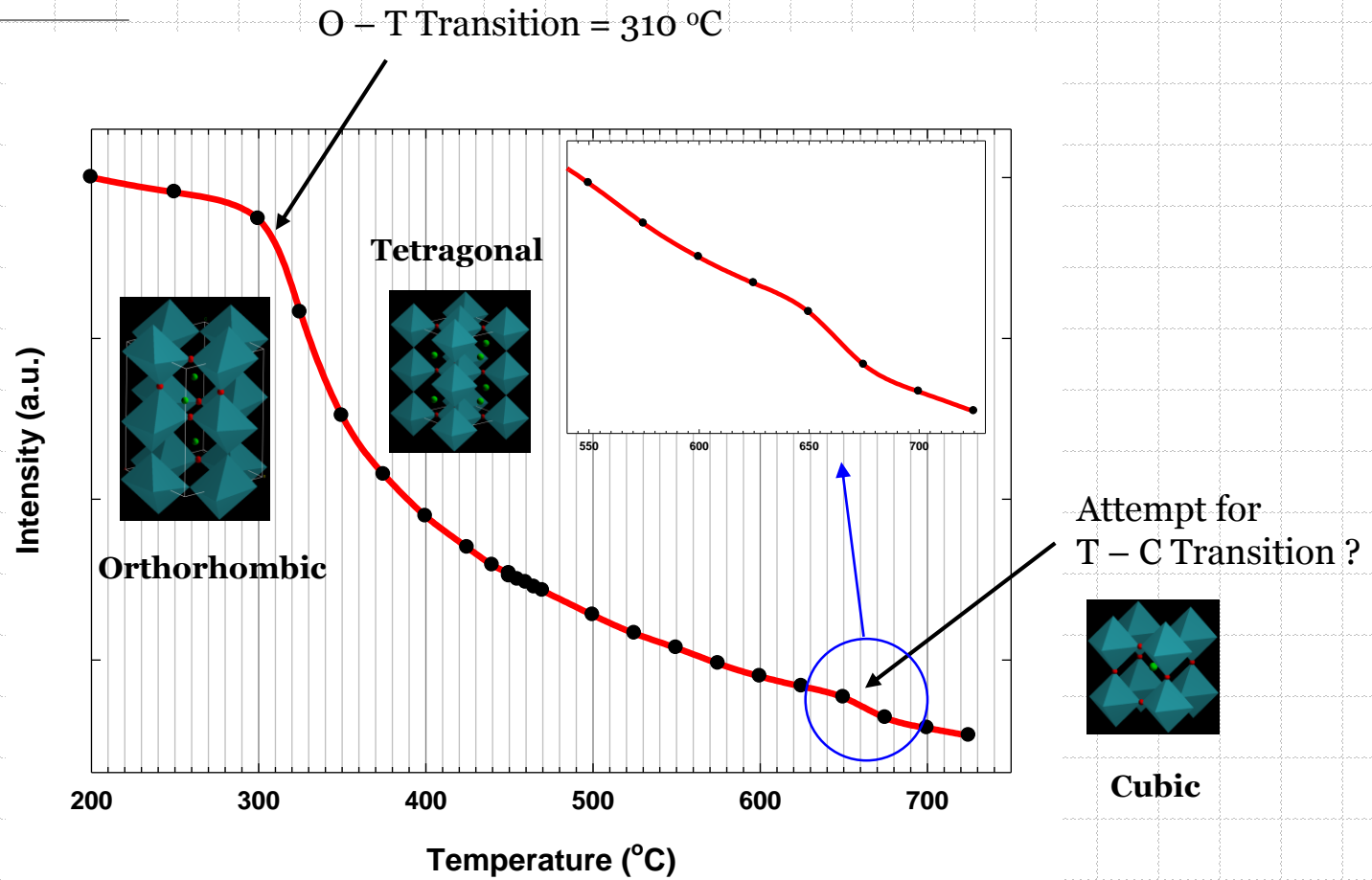
Structural Transition, (211) reflection



(211) peak is **absent** in cubic SrRuO_3

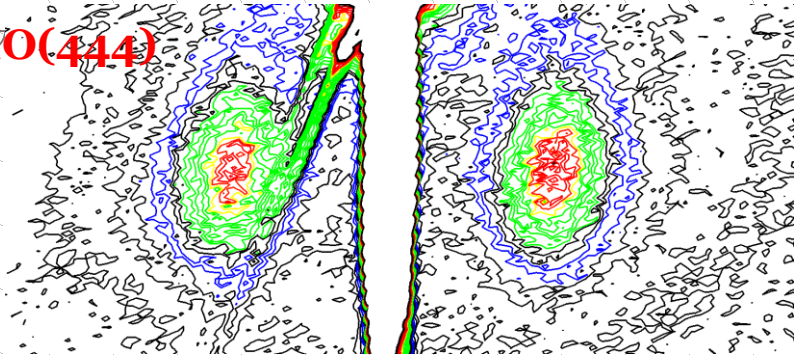


Structural Transition, (211) reflection



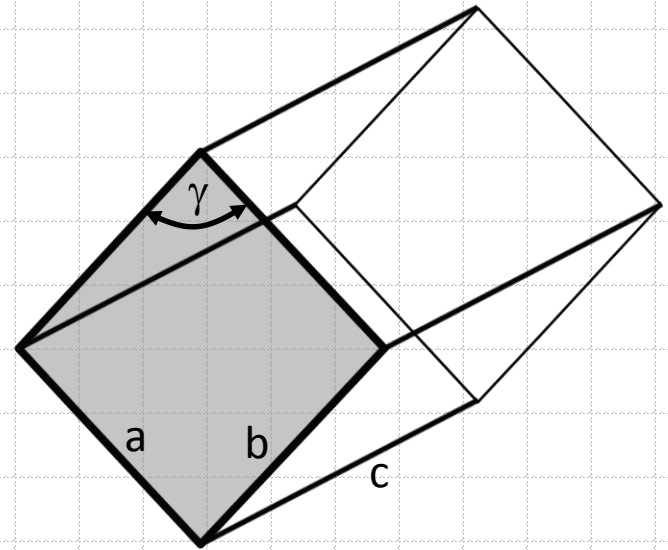
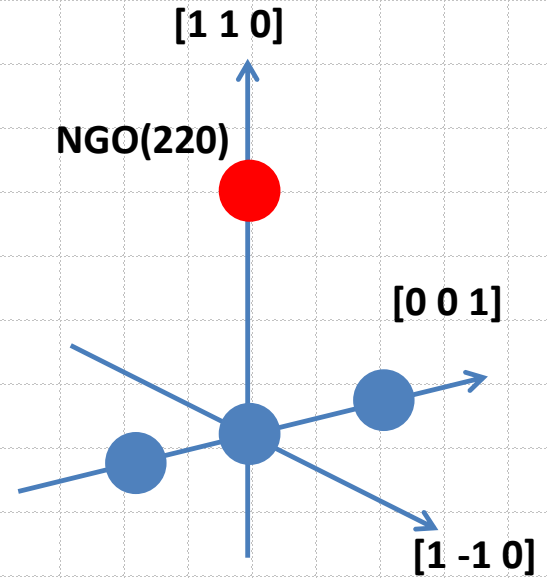
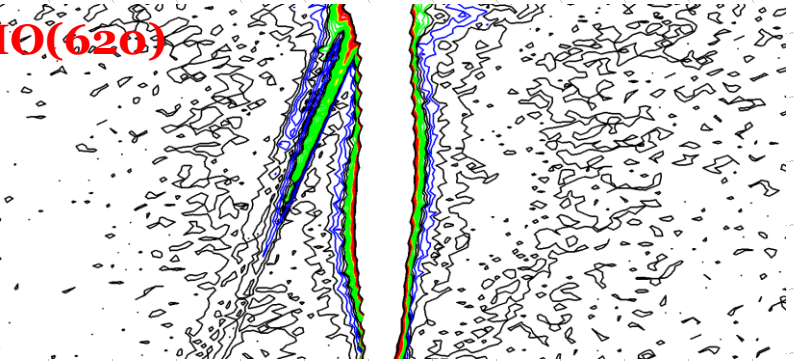
Beam along [001]

LSMO(444)



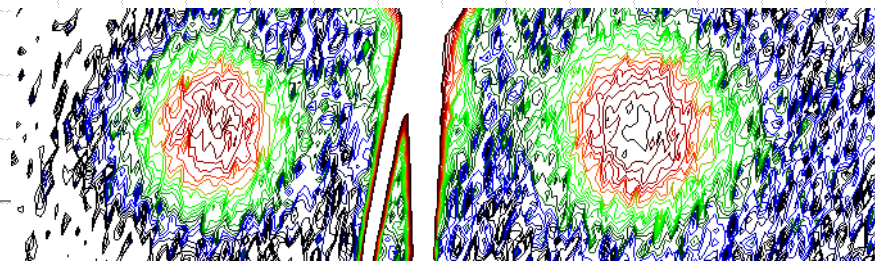
Beam along [1-10]

LSMO(620)

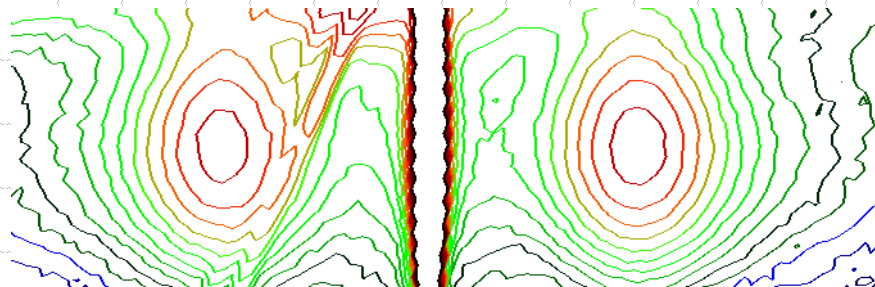


LSMO_NGO

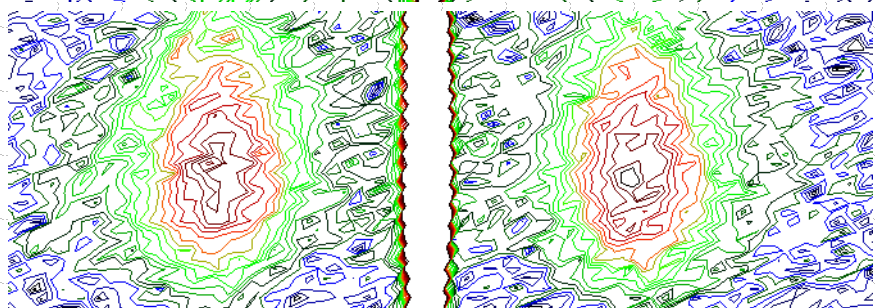
(110)



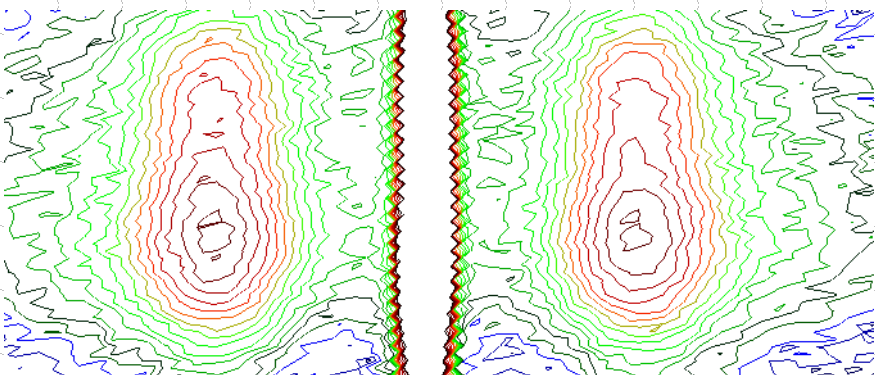
(220)



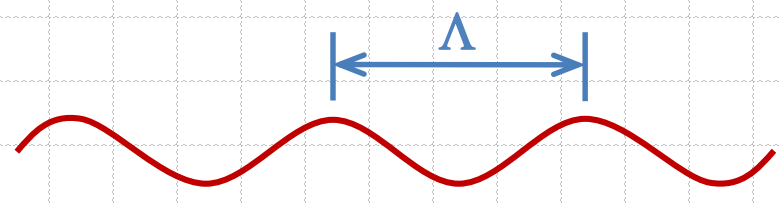
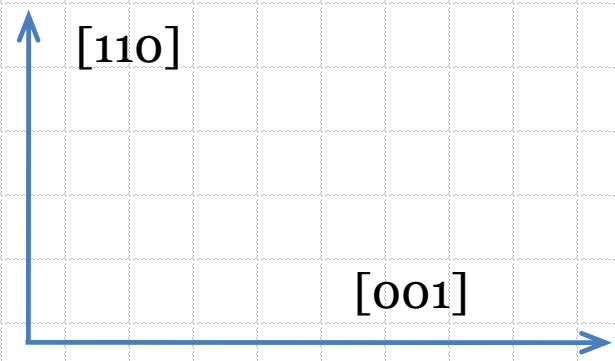
(330)



(440)



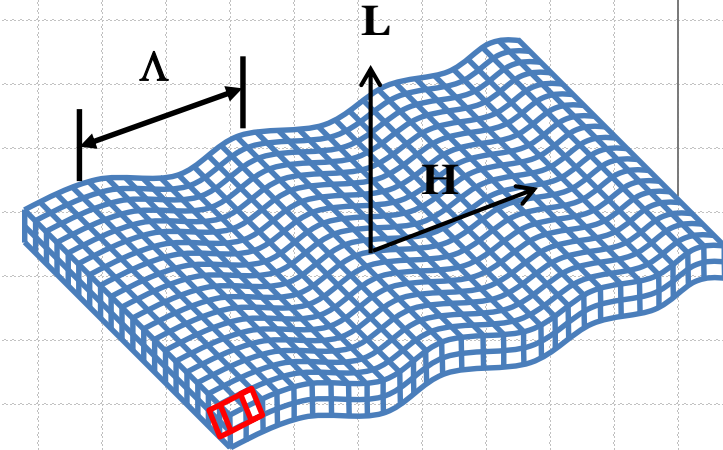
Satellite spacing does not change
along out-of-plane direction



The lattice modulations described using kinematical x-ray diffraction.

We used a cubic LSMO unit cell with $a_{c\parallel} = c/2$ and $a_{c\perp} = a^2 + b^2 - 2ab \cos(180 - \gamma)$

Unit cells have displacements along L-direction which are periodic along H-direction with periodicity, Λ . Then a one-dimensional complex structure factor along H-direction can be written as:



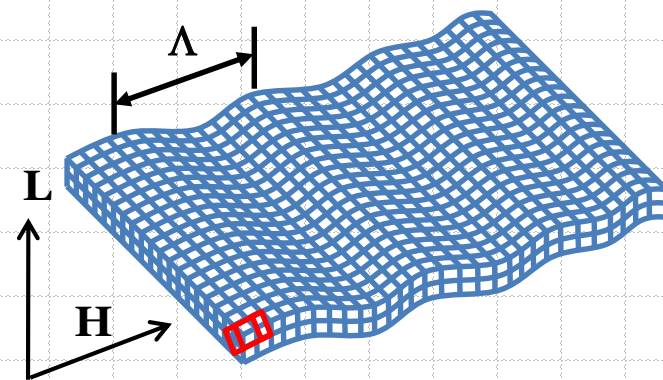
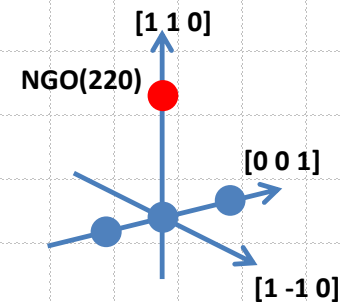
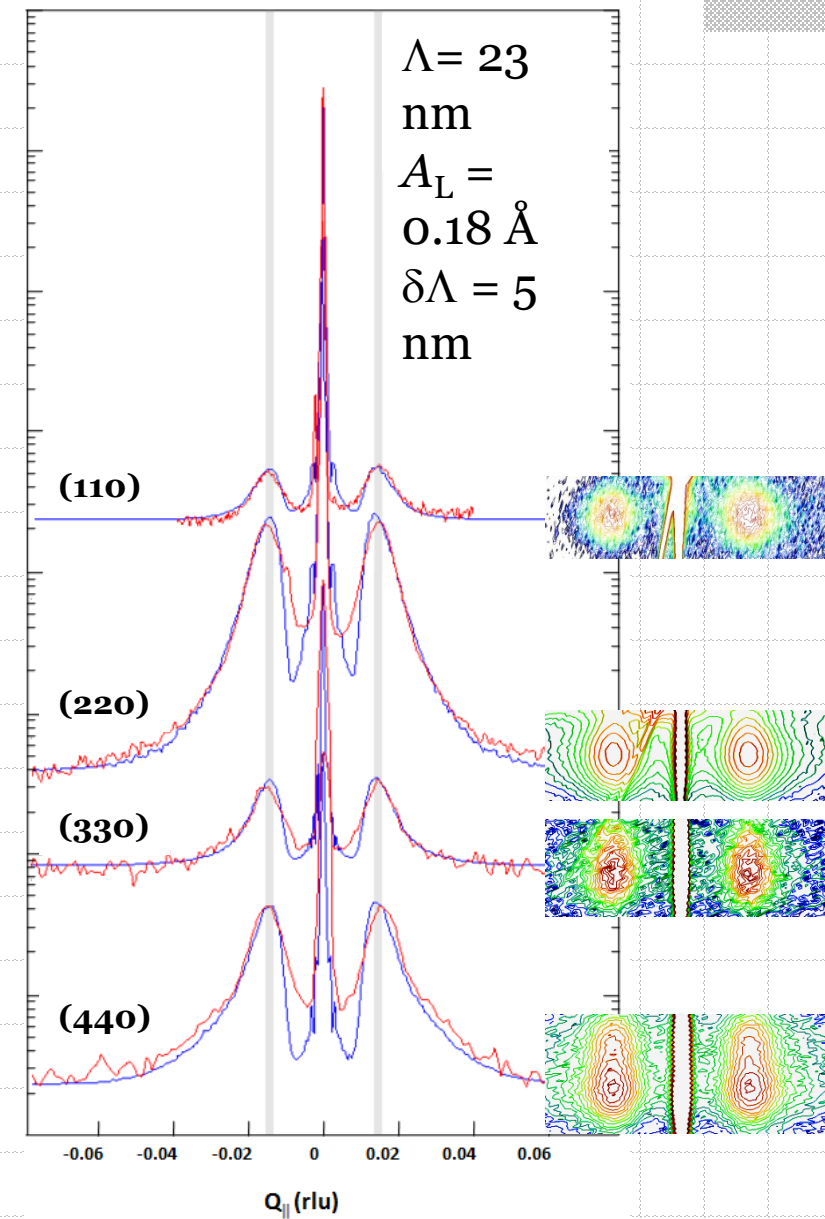
$$F_H = F_{uc} \sum_j e^{2\pi i(Hx_j + Lz_j)} = F_{uc} \sum_{n=1}^N e^{2\pi i\left(H\frac{x_n}{a_{c\parallel}} + L\frac{z_n}{a_{c\perp}}\right)}$$

$$F_{uc}, x_j = \frac{x_n}{a_{c\parallel}}, z_j = \frac{z_n}{a_{c\perp}}$$

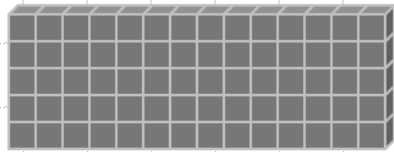
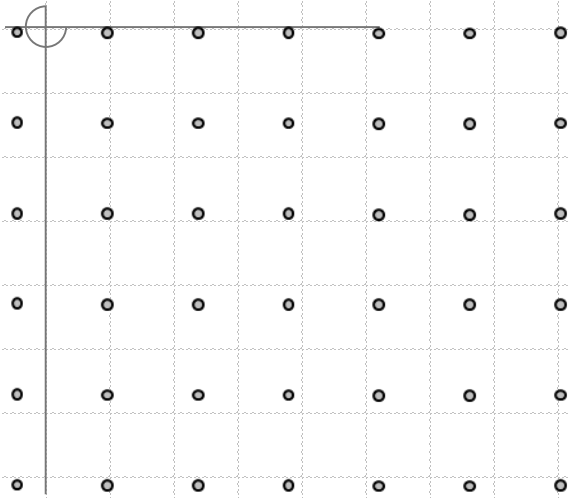
unit cell structure factor and relative x- and z-positions along H and L directions of a LSMO cubic unit cell

if $x_n = na_{c\parallel}$ and $z_n = A_L \cos(k_H na_{c\parallel})$ then:

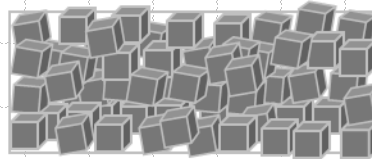
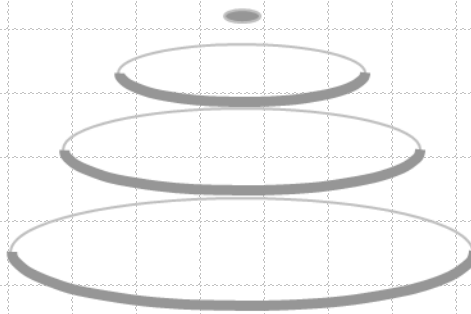
$$F_H = F_{uc} \sum_{n=1}^N e^{2\pi i\left[Hn + \frac{L}{a_{c\perp}} A_L \cos(k_H na_{c\parallel})\right]}$$



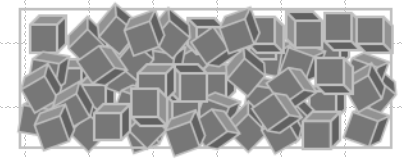
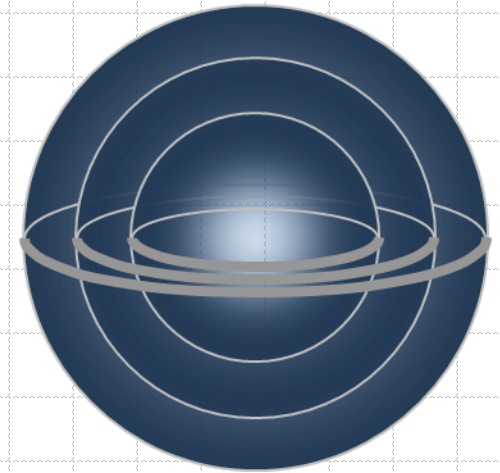
H-scans around LSMO(hko) reflections with $h = k = 1, 2, 3, 4$. The gray vertical lines are guides to the eye and show that satellite peaks originate from periodic atomic displacements and not from out-of-plane twinning.



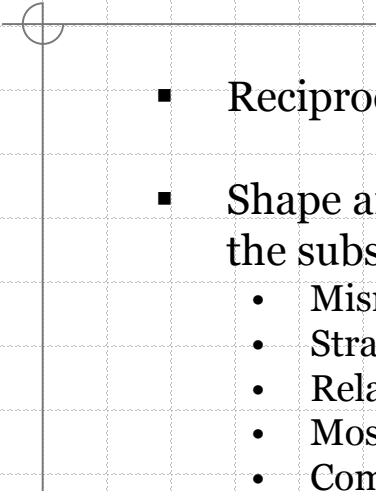
Single crystal



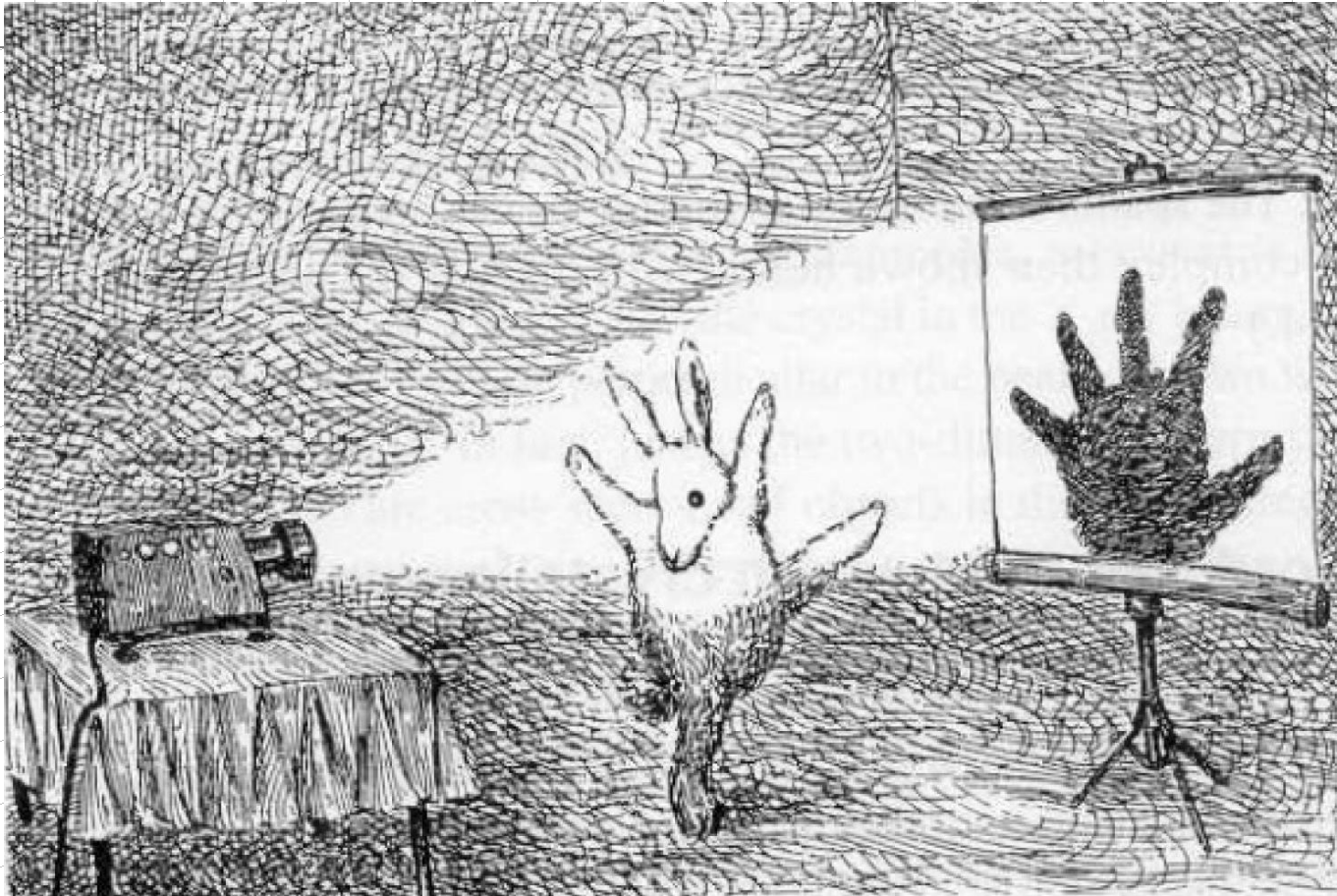
Preferred orientation



Polycrystalline

- 
- Reciprocal space for epitaxial thin films is very rich.
 - Shape and positions of reciprocal lattice points with respect to the substrate reveal information about:
 - Mismatch
 - Strain state
 - Relaxation
 - Mosaicity
 - Composition
 - Thickness
 - Diffractometer instrumental resolution has to be understood before measurements are performed.

Things can look very different in reciprocal space than in real space...



Fun in reciprocal space. © The New Yorker Collection, 1991. John O'Brien, from www.cartoonbank.com. All rights reserved.